The dynamics of spin-density waves

G. Grüner

Department of Physics and Solid State Science Center, University of California–Los Angeles, Los Angeles, California 90024

Spin-density waves (SDWs) are broken-symmetry ground states of metals, the name referring to the periodic modulation of the spin density with period, $\lambda_0=\pi/k_F$, determined by the Fermi wave vector k_F. The state, originally postulated by Overhauser, has been found in several organic linear-chain compounds. The development of the SDW state opens up a gap in the single-particle excitation spectrum, and the ground state is close to that of an antiferromagnet, as shown by a wide range of magnetic studies. Because of the magnetic ground state and of the incommensurate periodic spin modulation (which can be thought of as two periodic charge modulations in the two spin subbands), both collective charge and spin excitations may occur. These couple to ac magnetic and electric fields, which leads to antiferromagnetic resonances and frequency-dependent collective-mode conductivity. Both have been observed in the spin-density-wave ground state. The interaction of the collective mode with impurities pins the mode to the underlying lattice, and therefore the collective-mode charge excitations occur at finite frequencies in the long-wavelength limit. The mode can also be induced to execute a translational motion upon the application of a dc field which exceeds the threshold field E_T. Many of the observations on the ac, and on the nonlinear dc, response are similar to those which occur in materials with a charge-density-wave ground state. At low temperatures a novel type of collective transport suggestive of a tunneling process is observed. These low-temperature phenomena remain unexplained.

CONTENTS

I. Introduction 1
II. Organic Linear-Chain Materials: Model Compounds wi th a Spin-Density-Wave Ground State 2
III. The Spin-Density-Wave Transition and Ground State 4
  A. Mean-field theory of the spin-density-wave ground state 4
  B. Experimental evidence for the spin-density-wave ground state 7
IV. Collective Excitations 9
  A. Ginzburg-Landau theory of the excitations 9
  B. Collective magnetic excitations of the spin-density-wave state: antiferromagnetic-resonance experiments 10
V. Impurity Effects 11
VI. The Electrodynamics of Spin-Density Waves 13
  A. Models of the frequency-dependent conductivity 13
  B. Frequency-dependent conductivity of $(TMTSF)_2X$ salts 16
VII. Nonlinear Transport 18
  A. Nonlinear spin-density-wave conduction 18
  B. Current oscillations and interference effects 20
  C. Properties other than electrical conduction 21
  D. Nonlinear effects at low temperatures 22
VIII. Conclusions 23
Acknowledgments 23
References 23

I. INTRODUCTION

Spin-density waves are broken-symmetry ground states of metals which are thought to arise as the consequence of electron-electron interactions. The ground state is characterized by a periodic modulation of the spin density, the period being related to the Fermi wave vector k_F. This type of ground state was first proposed by Overhauser (1960, 1962) for isotropic metals. The spin-density-wave ground state, which will be discussed in this review, is somewhat different; it arises in highly anisotropic, so-called quasi-one-dimensional metals, and the ground state is schematically written as

$$\Delta\mathbf{S}(x)=\Delta\mathbf{S}_0\cos(2k_Fx+\phi)\ , \tag{1.1}$$

where $\Delta\mathbf{S}(x)$ denotes the spatially dependent spin modulation, which occurs along the chain direction x.

The spin-density-wave state has many similarities to other broken-symmetry ground states of metals, such as superconductivity and charge-density waves, and these states can be conveniently discussed within the framework of various one-dimensional models (see, for example, Solyom, 1979). Within the framework of a mean-field description, the ground states develop below a second-order phase-transition temperature, with the thermodynamics (within the framework of weak-coupling theories) the same as that of the BCS superconducting ground state. In all cases, a gap develops in the single-particle excitation spectrum, with the zero-temperature gap related (again within the framework of weak-coupling theory) to the transition temperature through the same relation $2\Delta=3.5kT_c$. In all cases, furthermore, the ground state is that of the coherent superposition of pairs, pairs of electrons for the superconducting state, pairs of electrons and holes with parallel spins for the charge-density-wave state, and pairs of electrons and holes with opposite spins for the spin-density-wave ground state. Consequently, the charge-density-wave ground state is nonmagnetic, while the spin-density-wave ground state has a well-defined magnetic character with associated low-lying magnetic excitations. These similarities and differences are clearly borne out by various experiments. Nor surprisingly, while the thermodynamics of these states are similar, density waves are in many respects different from superconductors, and this difference is most pronounced when the collective excitations and the dynamics of the ground states are examined. For both density waves, the low-lying charge exci-

 0034-6861/94/66(1)/1(24)/$07.40

tations are related to the spatial variations of the phase and are called phasons. In addition, in the spin-density-wave states, magnons are also the collective excitations of the ground state, which, as expected, is associated with two Goldstone modes, one with charge, and one with spin excitations. Another important difference lies in the coupling mechanism which leads to these ground states: charge-density waves occur primarily due to electron-phonon coupling, while the spin-density-wave state is due to electron-electron interactions. The consequence of the phonon degrees of freedom is the large dynamical mass, while for spin-density waves the dynamical mass is expected to be the same as the band mass. This difference has important consequences as far as screening effects and the electrodynamics are concerned. The small effective mass may also lead to quantum effects which are probably absent for charge-density waves. Some of the important characteristics of the ground states discussed above are summarized in Table I.

This review summarizes the current state of affairs of the field, with emphasis on the dynamics of spin-density waves. A short introduction to materials, organic linear-chain compounds that develop this ground state, is followed by a short summary of the basic features of the theory and parameters. The experimental evidence for a spin-density-wave state will be summarized next, and, not surprisingly, these experiments explore the magnetic character of the ground state. The collective excitations of the ground state are then reviewed with emphasis on the magnetic excitations sampled through antiferromagnetic-resonance measurements. The interaction of impurities with the spin-density-wave ground state (a topic that has many similarities to impurity–charge-density-wave interactions) is followed by the review of the electrodynamics of the ground state. The discussion of nonlinear transport, again with analogies to charge-density-wave transport, concludes this review.

The field is by no means a closed chapter of solid-state physics, and, in spite of spectacular progress, many important questions remain. Moreover, several important experiments have been performed on only a limited class of materials, and whether some of the properties found in a restricted group of materials are the universal features of this novel ground state remains to be seen.

II. ORGANIC LINEAR-CHAIN MATERIALS: MODEL COMPOUNDS WITH A SPIN-DENSITY-WAVE GROUND STATE

Planar organic molecules often form linear chains with large overlap of the π orbitals along the chain direction. When combined with counterions or molecules, the resulting charge-transfer salts may have partially filled bands leading to metallic properties. Members of these groups of materials, based on the organic molecules M shown in Fig. 1 and having the composition M_2X, also develop a spin-density-wave ground state at low temperatures.

The crystal structure of the material $(TMTSF)_2PF_6$ is shown in Fig. 2. The compound is composed of segregated stacks of TMTSF and PF_6 molecules. TMTSF is a good donor, and, when combined with good acceptors like PF_6 and similar species, a charge transfer occurs from the TMTSF stack to the acceptor stack; and for a full charge transfer (such as occurs for this compound), the TMTSF stack in the absence of anion ordering is $\frac{3}{4}$ filled. There is a significant overlap of the wave functions along the chain direction on the TMTSF stack, while the overlap is negligible along the PF_6 stack; consequently, band theory predicts metallic behavior dominated by the wave functions on the TMTSF stack along the chains. These materials indeed have metallic behavior down to low temperatures, as shown in Fig. 3 for $(TMTSF)_2PF_6$ (Bechgaard *et al.*, 1980). The increase of the resistivity below temperatures of about 20 K is due to the removal of the Fermi surface upon the formation of spin-density-wave ground states, as will be discussed later. The optical properties of $(TMTSF)_2PF_6$ are that of a Drude metal with high reflectivity along the chain direction, as shown in Fig. 4. From the analysis of the optical properties, the plasma frequency $\omega_p=(4\pi ne^2/m_b)$ can be extracted. This parameter is displayed in Table II. The magnetic susceptibility χ is of Pauli type and is temperature dependent down to low temperatures where the phase transition occurs (Mortensen *et al.*, 1981). The magnitude can then be used together with the known band filling to evaluate the parameters which characterize the metallic band along the chain direction. These parameters are also collected in Table II for the model compound $(TMTSF)_2PF_6$.

TABLE I. Various broken-symmetry ground states of one-dimensional metals.

	Pairing	Spin	Momentum	Broken symmetry	Low-lying collective excitations
Single superconductor	el-el	$S=0$	$q=0$	gauge	none
Triplet superconductor	el-el	$S=1$	$q=0$	gauge	?
Charge-density wave	el-hole	$S=0$	$q=2k_F$	translational	phasons amplitudons
Spin-density wave	el-hole	$S=1$	$q=2k_F$	translational	phasons magnons

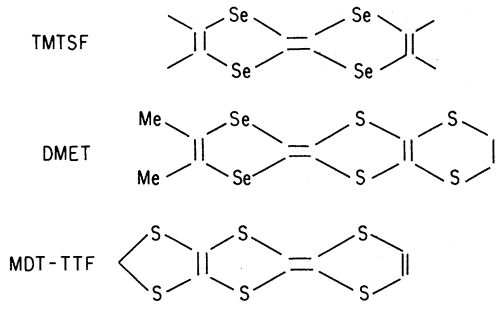

FIG. 1. Several planar organic acceptor molecules that form metallic charge-transfer salts and a spin-density-wave ground state.

The electrical conductivity is highly anisotropic, and σ, when measured perpendicular to the chain directions, is small, indicating a transfer integral smaller than the thermal energy kT (except at low temperatures) in these directions. This then implies nonmetallic behavior perpendicular to the chains. This conclusion is supported by optical studies. The reflectivity measured in $(TMTSF)_2PF_6$ along one direction perpendicular to the chain (the b-axis) direction, displayed as curve $E\|b$ in Fig. 4, does not show a plasma edge as would be expected for a metallic band at high temperatures. However, such a plasma edge is observed below about 60 K. From optical conductivity and NMR studies, bandwidths of approximately 80 meV and 10 meV are inferred for the two

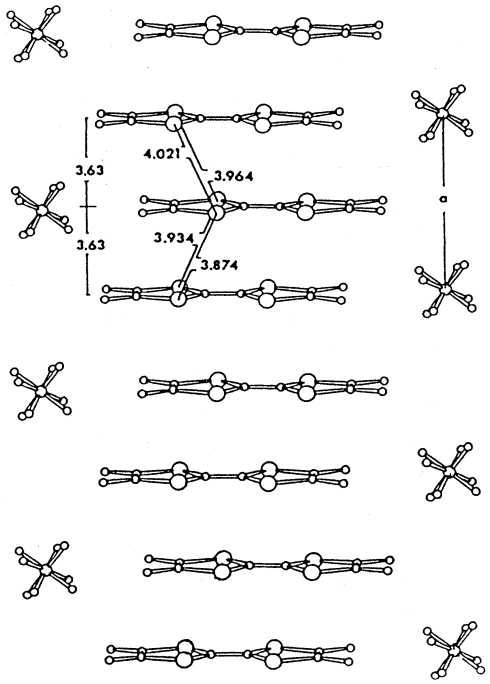

FIG. 2. Crystal structure of (tetramethyltetraselenofulvalene)$_2PF_6$, $(TMTSF)_2PF_6$. The Se-Se distance is indicated in Å.

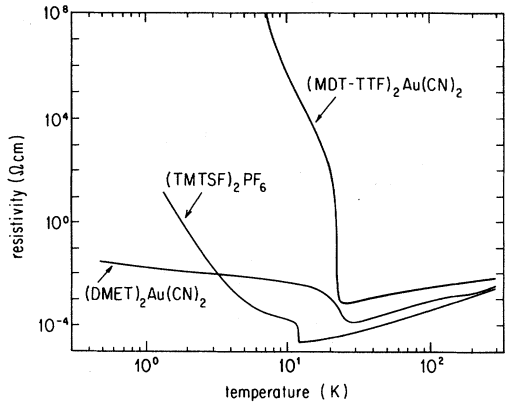

FIG. 3. dc electrical resistivity of various organic M_2X salts which develop a spin-density-wave ground state at low temperatures. The DMET results are taken from Honda *et al.* (1989), and the other measurements were made at UCLA.

perpendicular directions (Jérome and Schultz, 1982). In contrast, the bandwidth along the chain direction is approximately 1 eV, significantly larger than the thermal energy.

Members of other groups of organic linear-chain compounds have also been found to develop a spin-density-wave ground state. The organic salts, $(MDTTF)_2X$, where MDTTF stands for methylendithio-tetrathiafulvalene (the molecule is displayed in Fig. 1), have a crystal structure again formed of segregated stacks of donors and acceptors with a partially filled band along the donor stacks as the consequence of charge transfer. Several members of this group have metallic character for various counterions, and one member of the group $(MDTTF)_2Au(CN)_2$ has a spin-density-wave transition at

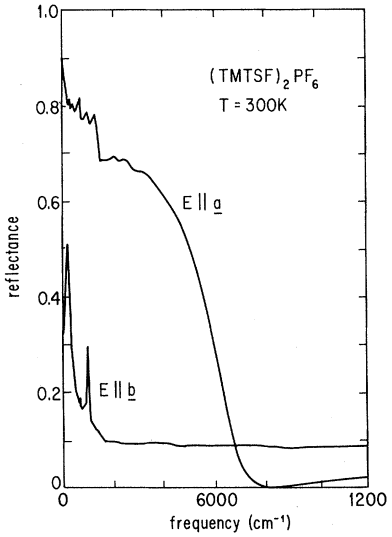

FIG. 4. Optical reflectance of $(TMTSF)_2PF_6$ at room temperature with the electric field both parallel ($E\|a$) and perpendicular ($E\|b$) to the chain direction (Jacobsen *et al.*, 1982).

TABLE II. Parameters of the metallic state of materials with a spin-density-wave ground state. The electron density has been evaluated from the band filling and from the crystal structure parameters.

	Band filling	χ (10^{-6} emu/mole)	$\hbar\omega_p$ (eV)	$\frac{m_b}{m_e}$	ε_F	V_F (10^7 cm/sec)	$n(\varepsilon_F)$ (eV^{-1})
$(TMTSF)_2PF_6$	1/4	0.58[a]	2.9[b]	1.3 2.4	6.1	0.86	0.25
$(DMET)_4Au(CN)_2$	1/4	0.51[c]		2.4	6.6	1.0	0.26

[a]Mortensen *et al.* (1982); Jérome and Schultz (1982).
[b]Jacobsen *et al.* (1983).
[c]Kanoda *et al.* (1988).

low temperatures (Nakamura *et al.*, 1990). This leads to the increase of the resistivity, as shown in Fig. 3, as the development of the SDW state leads to the removal of the Fermi surface. Like the TMTSF family, the band structure is anisotropic, as expected from the anisotropic overlap of the wave functions. The parameters of the single-particle states have not, however, been evaluated for this group of materials.

The molecule dimethylethylenedithio-diselenadithiafulvalene, DMET, also forms various charge-transfer salts with different counterions, and the composition is $(DMET)_2X$. The structural features of these compounds are similar to those of the previous two groups of materials. Some members of this family are semiconductors, while other members remain metals to low temperatures where they undergo transitions to various broken-symmetry states (Kikuchi *et al.*, 1987). In the compound $(DMET)_2Au(CN)_2$, the ground state is that of a spin-density wave, as will be discussed later.

Because of the small specimen dimensions, optical studies have, in general, not been performed on these materials. The magnetic susceptibility, too, has been measured in only a few cases. Consequently, the parameters of the single-particle band have been evaluated only for a few compounds, which are collected in Table II.

III. THE SPIN-DENSITY-WAVE TRANSITION AND GROUND STATE

The spin-density-wave ground state of metals is thought to arise as a consequence of electron-electron interactions. Questions on the detailed nature of this interaction and also the consequences of this interaction on the Fermi-liquid state have received considerable attention, and there is a vast literature on the various ground states which develop.

The simplest possible description of this interaction is given by the term

$$H_{\rm int}=\frac{U}{N}\sum_{q,\sigma}n_{q,\sigma}n_{-q,-\sigma}=\frac{U}{N}\sum_{k,k',q}a^{\dagger}_{k,\sigma}a_{k+q,\sigma}a^{\dagger}_{k',-\sigma}a_{k'-q,-\sigma}\ , \tag{3.1}$$

where U is the on-site Coulomb interaction and N is the number of electrons per unit length. Together with the kinetic-energy terms, the so-called Hubbard Hamiltonian is given in one dimension by

$$H=\sum_{k\sigma}\varepsilon_k a^{\dagger}_{k\sigma}a_{k\sigma}+\frac{U}{N}\sum_{k,k',q}a^{\dagger}_{k,\sigma}a_{k+q,\sigma}a^{\dagger}_{k',-\sigma}a_{k'-q,-\sigma}\ . \tag{3.2}$$

As will be discussed later, the ground state of Eq. (3.2) is that of a spin-density-wave state, and the transition together with the parameters of the state will be described within the framework of a mean-field theory. It is assumed that $U\ll\varepsilon_F$, which is equivalent to the weak-coupling limit for superconductors. The development of the ground state opens up a gap at the Fermi level; consequently, in the case of the complete removal of the Fermi surface (such as expected for a highly anisotropic band structure), a metal-insulator transition results. The ground state also has a well-defined magnetic character. Consequently, transport and magnetic measurements, together with local probes which sample the internal magnetic fields at the nuclear sites, have been used to evaluate the essential characteristics of the ground state.

A. Mean-field theory of the spin-density-wave ground state

The interaction between the electrons with opposite spin, as given by Eq. (3.1), leads to an enhanced response to an external magnetic field. This response can be simply described by using the mean-field approximation. Assume that we apply an external magnetic field that varies along the chain direction as

$$H(x)=\sum_q H_q e^{iqx}\ . \tag{3.3}$$

The coupling to this field is described by an extra term in the Hamiltonian

$$H'=-\sum_q M_q H_{-q}\ , \tag{3.4}$$

where M_q is the qth component of the magnetization. Assume that the magnetic field is applied to the (arbitrarily

chosen) z direction. The spin direction parallel (opposite) to H is denoted by $\uparrow(\downarrow)$. Then the expectation value of the magnetization is

$$\langle M_q \rangle = \mu_B(\langle n_{q,\uparrow} \rangle - \langle n_{q,\downarrow} \rangle) = N\chi_0(q)H_q^{\text{eff}} \tag{3.5}$$

with

$$H^{\text{eff}} = H_q + \frac{U(\langle n_{q,\uparrow} \rangle - \langle n_{q,\downarrow} \rangle)}{2\mu_B} , \tag{3.6}$$

where $X_0(q)$ is the susceptibility in the absence of Coulomb interactions. The self-consistent equation for the difference $\Delta n_q = \langle n_{q,\uparrow} \rangle - \langle n_{q,\downarrow} \rangle$ then is

$$\mu_B \Delta n_q = N\chi_0(q)\left[H_q + \frac{U\Delta n_q}{2\mu_B N}\right] . \tag{3.7}$$

The magnetization from Eqs. (3.5) and (3.7) is

$$\langle M_q \rangle = \frac{N\chi_0(q)}{1 - U\chi_0(q)/2\mu_B^2} H_q = N\chi(q)H_q , \tag{3.8}$$

and the enhanced response is given by an enhanced susceptibility

$$\chi(q) = \frac{\chi_0(q)}{1 - U\chi_0(q)/2\mu_B^2} . \tag{3.9}$$

For a uniform magnetization, $q=0$, and with $\chi_0(0) = 2\mu_B^2 n(\varepsilon_F)$, one obtains a static susceptibility

$$\chi(0) = \frac{2\mu_B^2 n(\varepsilon_F)}{1 - Un(\varepsilon_F)} , \tag{3.10}$$

enhanced by the well-known Stoner factor. For a one-dimensional electron gas, $\chi_0(q)$ is strongly peaked at $q = 2k_F$, and the enhancement is most important for perturbation with this wave vector. $\chi_0(2k_F, T)$ is in one dimension strongly temperature dependent. It is given by $\chi_0(2k_F, T) = n(\varepsilon_F)\ln(\varepsilon_0/kT)$ with ε_0 a cutoff energy, on the order of the Fermi energy ε_F. This feature leads to a strongly temperature-dependent enhanced response, and (with fluctuation effects neglected) to the phase transition at temperature $T_{\text{SDW}}^{\text{MF}}$ defined as

$$\frac{U\chi_0(2k_F, T)}{2\mu_B^2} = Un(\varepsilon_F)\ln\frac{1.14\varepsilon_0}{k_B T} = 1 , \tag{3.11a}$$

which gives

$$k_B T_{\text{SDW}}^{\text{MF}} = 1.14\varepsilon_F \exp\left[-\frac{1}{\lambda}\right] , \tag{3.11b}$$

where the dimensionless electron-electron coupling constant is defined as

$$\lambda = Un(\varepsilon_F) . \tag{3.12}$$

Below $T_{\text{SDW}}^{\text{MF}}$ a static, spatially varying magnetization develops. By introducing the spatially dependent operators

$$\psi_\sigma(x) = \frac{1}{\sqrt{V}}\sum_k e^{ikx} a_{k,\sigma} , \tag{3.13}$$

the spin density is given as

$$S(x) = \frac{1}{2}[\psi_\uparrow^\dagger(x)\psi_\uparrow(x) - \psi_\downarrow^\dagger(x)\psi_\downarrow(x)] \tag{3.14}$$

$$= \frac{1}{2V}\sum_{k,k'}\{a_{k\uparrow}^\dagger a_{k'\uparrow} - a_{k\downarrow}^\dagger a_{k',\downarrow}\}e^{-i(k-k')x} . \tag{3.15}$$

Because of the divergent response function at $q = 2k_F$, we assume that only terms with $k' = k \pm 2k_F$ are important. Thus the above equation yields

$$\langle S(x) \rangle = \frac{1}{2V}\sum_k \{\langle a_{k,\uparrow}^\dagger a_{k+2k_F,\uparrow} \rangle - \langle a_{k,\downarrow}^\dagger a_{k+2k_F,\downarrow} \rangle\} e^{+i2k_F x} + \text{c.c.} \tag{3.16}$$

We write the expectation values as

$$\begin{aligned} S = |S|e^{i\phi} &= \frac{1}{V}\langle n_{2k_F\uparrow} \rangle = \frac{1}{V}\sum_k \langle a_{k,\uparrow}^\dagger a_{k+2k_F,\uparrow} \rangle \\ &= \frac{1}{V}\sum_k \langle a_{k,\downarrow}^\dagger a_{k+2k_F,\downarrow} \rangle \\ &= -\frac{1}{V}\langle n_{2k_F\downarrow} \rangle , \end{aligned} \tag{3.17}$$

assuming that there is no charge-density modulation associated with the ground state. From Eq. (3.16) we obtain

$$\langle S(x) \rangle = 2|S|\cos(2k_F x + \phi) . \tag{3.18}$$

Therefore the spin density is spatially varying, with a period, $\lambda_0 = \pi/k_F$, determined by the Fermi wave vector.

Using the standard mean-field approximation, the magnetic moment μ is

$$\langle \mu \rangle = g\mu_B \langle S \rangle = 2\mu_B \langle S \rangle , \tag{3.19}$$

and therefore the spatially dependent magnetic moment is written as

$$\langle \mu(x) \rangle = \mu_0 \cos(2k_F x + \phi) , \tag{3.20}$$

where $\mu_0 = 4\mu_B S$. We define a complex order parameter

$$\Delta e^{i\phi} = \frac{U}{N} S , \tag{3.21}$$

and then the mean-field Hamiltonian becomes (dropping a constant Hartree energy)

$$H_{\text{MF}} = \sum_{k\sigma}\varepsilon_k a_{k\sigma}^\dagger a_{k\sigma} + \frac{2N}{U}|\Delta|^2 + \left\{\sum_k \Delta e^{i\phi}(a_{k+2k_F,\uparrow}^\dagger a_{k,\uparrow} + a_{k+2k_F,\downarrow}^\dagger a_{k,\downarrow}) + \text{H.c.}\right\} . \tag{3.22}$$

Straightforward diagonalization leads to

$$H = \sum_{k,\sigma} E_k \gamma_{k\sigma}^\dagger \gamma_{k\sigma} + 2N\frac{|\Delta|^2}{U} \tag{3.23}$$

with the dispersion relation of the operators $\gamma_{k\sigma}$ given by

$$E_k=\varepsilon_F+\mathrm{sgn}(|k|-k_F)[\hbar^2V_F^2(|k|-k_F)^2+|\Delta|^2]^{1/2} . \tag{3.24}$$

The development of the single-particle gap leads to a decrease of the kinetic energy, while the interaction term $2|\Delta|^2/U$ [the second term in Eq. (3.22)] gives a positive energy for a finite magnetization. The equilibrium gap value is obtained from

$$\delta E_{\mathrm{el}}+\delta E_M=0 , \tag{3.25}$$

where δE_M is the energy associated with the second term on the right-hand side of Eq. (3.23). Straightforward algebra gives

$$\Delta(T=0)=2\varepsilon_F \exp\left[-\frac{1}{\lambda}\right] . \tag{3.26}$$

A comparison with Eq. (3.11b) leads to the weak-coupling BCS relation $2\Delta=3.52k_BT_{\mathrm{SDW}}^{\mathrm{MF}}$, and the ground-state energy is given by

$$E=-\tfrac{1}{2}n(\varepsilon_F)|\Delta|^2 . \tag{3.27}$$

The temperature dependence of the single-particle gap, and hence the amplitude of the spin-density wave, are given by the weak-coupling BCS expression (see, for example, Tinkham, 1975).

Crudely speaking, the SDW ground state can be viewed as two charge-density-wave states—one for the "spin-up" and one for the "spin-down" sub-bands as shown in Fig. 5, with the charge-density-wave modulations given by

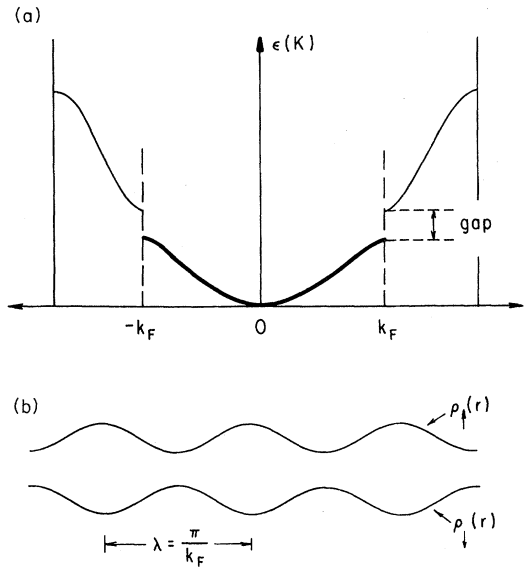

FIG. 5. The spin-density-wave state. (a) The dispersion relation for a one-dimensional SDW material below the phase transition. The opening of the gap at $\pm k_F$ is clearly visible. (b) A SDW viewed as two CDWs—one for the spin-up subband and another for the spin-down—which are spatially out of phase by π.

$$\rho_\uparrow(x)=\rho_0\left[1+\frac{\Delta}{V_Fk_F\lambda}\cos(2k_Fx+\phi)\right] , \tag{3.28a}$$

$$\rho_\downarrow(x)=\rho_0\left[1+\frac{\Delta}{V_Fk_F\lambda}\cos(2k_Fx+\phi+\pi)\right] , \tag{3.28b}$$

where the coupling constant $\lambda=Un(\varepsilon_F)$.

The resulting spin-density variation $\rho_\uparrow(x)-\rho_\downarrow(x)$ is given by Eq. (3.18) with $|S|=\Delta N/U$ [see Eq. (3.21)], and the resulting charge-density-wave variation $\rho_\uparrow+\rho_\downarrow=\rho_0$ is shown in Fig. 5. Both subbands, however, are tied to the Fermi surface, and this will have important implications on the excitations and on the dynamics of the SDW ground state.

The above considerations are for an arbitrary spin orientation; in the case of a continuous spin symmetry, the condensate density can be written as

$$\langle \mathbf{S}(x)\rangle=\mathbf{S}_0\cos(2k_Fx+\phi) \tag{3.29}$$

where $\mathbf{S}=(S_x,S_y,S_z)$. Consequently both the spin rotation and the translational symmetry are broken in the spin-density-wave state. This will have important consequences on the magnetic properties of the ground state and on the dynamics of the collective mode.

The description of the SDW transition and ground state as given above is based on a strictly one-dimensional model. The materials that develop a SDW ground state have, however, significant transfer integrals perpendicular to the chain directions, and models which include this so-called quasi-one-dimensional character are expected to be more appropriate. Taking into account the finite bandwidth in the perpendicular directions, the dispersion relation is given by (Yamaji, 1982, 1983; Huang and Maki, 1990)

$$\varepsilon_k=-2t_a\cos(ak_1)-2t_b\cos(bk_2)-2t_c\cos(ck_3)-\mu , \tag{3.30}$$

where μ is the chemical potential, and t is the transfer integral in the various directions. For $t_a\gg t_b,t_c$, the condition for nesting,

$$\varepsilon_k=\varepsilon_{k+Q} \tag{3.31}$$

with $Q=(2k_F,\pi/b,\pi/c)$, is nearly, but not entirely, satisfied. This leads to deviations from the various expressions which have been obtained on the basis of strictly one-dimensional models. The transition temperature T_{SDW} decreases with increasing transfer integral perpendicular to the chain direction, and the transition is completely removed for

$$\Delta(T=0)-\mu_0=\frac{t_b^2}{2t_a}\cos ak_F\sin^2 ak_F \tag{3.32}$$

with $\Delta(T=0)$ given by Eq. (3.26). In addition, the spin-density-wave modulation is given by

$$\Delta\mathbf{S}(\mathbf{r})=\Delta\mathbf{S}_0\cos(\mathbf{Q}\cdot\mathbf{r}+\phi) \tag{3.33}$$

with $\mathbf{Q}=(2k_F,\pi/b,\pi/c)$.

B. Experimental evidence for the spin-density-wave ground state

Evidence for transitions to spin-density-waves states has been found in several members of organic linear-chain compounds that have been discussed in Sec. II. Measurements of the various thermodynamic quantities have been performed in only a few cases, and the principal observations on the transition are those of the transport and magnetic properties.

As for charge-density waves, the development of the SDW ground state opens up a gap at the Fermi level, leading to metal-insulator transitions. The dc conductivity measured on three compounds that develop a SDW ground state is displayed in Fig. 6. In all three cases there is a well-defined transition from metallic to semiconducting behavior; and as for charge-density waves, the transition temperatures, called T_{3D}, are identified through the measurement of the temperature derivative $d\ln\rho/d(1/T)$. Below T_{3D}, the conductivities are well described by

$$\sigma=\sigma_0\exp\left[-\frac{\Delta}{kT}\right]. \tag{3.34}$$

The single-particle gaps, evaluated using Eq. (3.34), together with the transition temperatures, are collected in Table III. These values, together with the parameters that characterize the metallic state above T_{3D}, lead, using Eq. (3.12), to the coupling constant λ.

At low temperatures deviations from the Arrhenius behavior are observed. These are most probably due to hopping conduction due to impurity states in the gap.

The density of states above the transition, $n(\varepsilon_F)$, has been evaluated from the magnetic susceptibility, and the values given in Table II lead from Eqs. (3.11) and (3.12) to the Coulomb energies displayed in Table III, which

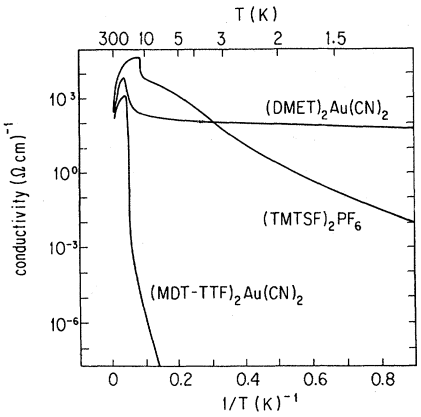

FIG. 6. Temperature dependence of the dc conductivity vs the inverse temperature for various compounds with a SDW ground state at low temperatures.

are smaller than ε_F. In all compounds, therefore, Coulomb effects lead in these materials to a SDW state, in the so-called weak coupling limit. The measured single-particle gap, together with the Fermi velocities, also leads to large coherence lengths, and the zero-temperature values $\xi_{0\|}=\hbar V_F/\pi\Delta$ are also given in Table III. As for charge-density waves, because of the strongly anisotropic bandwidth in the various crystallographic directions, the coherence length is also anisotropic. This anisotropy has been measured only for some of the $(TMTSF)_2X$ salts; and with the anisotropic Fermi velocities, as discussed in Sec. II, one obtains

$$\xi_{\perp y}\simeq 30\ \text{Å}\ , \tag{3.35a}$$

$$\xi_{\perp z}\simeq 1\ \text{Å}\ . \tag{3.35b}$$

The above values of the single-particle gaps and Coulomb energies also suggest small magnetic moments associated with the spin-density-wave state. The amplitude of the SDW modulation may be written as

$$\frac{\mu}{\mu_B}=\frac{4|\Delta|}{U} \tag{3.36}$$

TABLE III. Parameters of the spin-density-wave state in various compounds: Δ_ρ refers to the single-article gap as evaluated from the temperature dependence of the dc resistivity.

	$T_{SDW}(k)$	$\Delta_\rho(\kappa)$	λ [Eq. (3.11)]	ξ(Å)	$\frac{\mu}{\mu_B}$ (NMR)	$\frac{\mu}{\mu_B}$ [Eq. (3.36)]	U (eV) [Eq. (3.12)]
$(TMTSF)_2PF_2$	11.5[a]	15	0.26	320	0.08[b,c]	0.01	2.0
$(MDT\text{-}TTF)_2Au(CN)_2$	20[d]				0.1[e]		2.0
$(DMET)_2Au(CN)_2$	20[f]	100	0.25	160	0.1[g]	0.008	2.0

[a]Jérome and Schultz (1982).
[b]Takahashi *et al.* (1986a, 1986b).
[c]Delrieu, Roger, Toffano, Wope Mbougue, *et al.* (1986).
[d]Nakamura *et al.* (1990).
[e]Kanoda *et al.* (1990).
[f]Kikuchi *et al.* (1987).
[g]Kanoda *et al.* (1988).

with μ_B the Bohr magneton. The values of Δ and U as evaluated above lead to the reduced magnetic moments and are given in Table III. The magnetic properties of the SDW state in the weak-coupling limit have not been calculated. It is expected that the magnetic response and the collective excitation are close to that of an antiferromagnet with a reduced moment and effective exchange constant J_{eff}. Therefore the Hamiltonian

$$\mathcal{H}=\left[\frac{\mu}{\mu_B}\right]^2 J_{\text{eff}}\sum_i \mathbf{S}_i\mathbf{S}_{i+1}-\left[\frac{\mu}{\mu_B}\right]^2 D\sum_i S_i^x S_{i+1}^x + \left[\frac{\mu}{\mu_B}\right]^2 E\sum_i (S_i^z S_{i+1}^z - S_i^y S_{i+1}^y) - g\mu_B \mathbf{H}\sum_i \mathbf{S}_i \quad (3.37)$$

has been used to evaluate the parameters that characterize the SDW ground state. Here J_{eff} is an effective antiferromagnetic interaction along the chains; D represents the hard-axis anisotropy; and E the intermediate-axis anisotropy. The reduced moment is written as μ/μ_B, and the easy, intermediate, and hard axes are z, y, and x, respectively. The above Hamiltonian leads to an anisotropic susceptibility, with

$$\chi_{\parallel}\rightarrow 0 , \quad (3.38a)$$

$$\chi_{\perp}=\frac{Ng^2\mu^2}{2(\mu/\mu_B)2J_{\text{eff}}}=\frac{Ng^2\mu_B^2}{2J_{\text{eff}}} \quad (3.38b)$$

at zero temperature. Here the parallel direction refers to the magnetic field, which is applied parallel to the axis along which the electron spins are aligned in the absence of an external magnetic field.

This anisotropy has been observed in $(TMTSF)_2X$ salts,

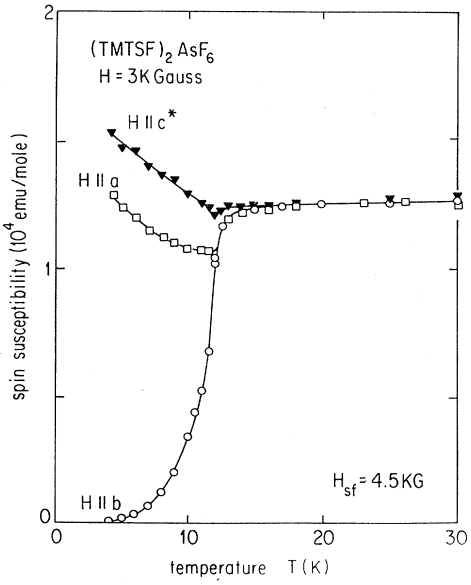

FIG. 7. Temperature dependence of the single-crystal spin susceptibility of $(TMTSF)_2AsF_6$ in a magnetic field ($H=3$ kOe) lower than the spin-flop field. The axes b, a, and c^* are, respectively, the easy, intermediate, and hard axes of the SDW state stable below 12 K after Ref. ?).

and the susceptibility measured (Mortensen *et al.*, 1981, 1982) in the AsF_6 salt is displayed in Fig. 7. The magnitude of $\chi_{\perp}$ leads, using Eq. (3.38b), to an effective coupling constant $J_{\text{eff}}=1400$ K. The Hamiltonian, Eq. (3.37), also leads to a spin-flop field, whose value is

$$H_{sf}=\frac{\pi(2EJ_{\text{eff}})^{1/2}}{\hbar\gamma} , \quad (3.39)$$

where γ is the gyromagnetic ratio. Experiments at various magnetic fields, again in $(TMTSF)_2X$ salts (Mortensen *et al.*, 1982), clearly establish the existence of a spin-flop field, which is of the order of $H_{sf}=4.5$ kG from which an anisotropy energy of $E=3\times10^{-5}$ K has been estimated.

The spatial variation of the spin density, as given by Eq. (3.18), leads to a spatial variation of the internal field at the nuclear sites given by

$$\delta H(x)=\langle a_0\rangle H_0\frac{\mu}{\mu_B}\cos(2k_F x+\phi) \quad (3.40)$$

in the presence of an external dc magnetic field H_0, where $\langle a_0\rangle$ is the hyperfine field interaction (a quantity which, in general, can be estimated). The internal field distribution, which is a sensitive function of the precise spatial dependence of the spin density, can be measured by local probes such as nuclear magnetic resonance (NMR) and muon spin rotation (μSR). Note that for a commensurate SDW, the distribution of the local field at the nuclear sites is different from the distribution caused by an incommensurate SDW. Consequently such studies can establish the incommensurate character of the density wave, and an elaborate analysis can also establish the nesting wave vector, $\mathbf{Q}=(Q_{\perp},2k_F)$. This has been done for $(TMTSF)_2PF_6$ (Andrieux *et al.*, 1981; Creuzet *et al.*, 1982; Takahashi *et al.*, 1984, 1986a, 1986b; Delrieu, Roger, Toffano, Moradpour, and Bechgaard, 1986; Delrieu, Roger, Toffano, Wope Mbougue, *et al.*, 1986), leading to a SDW distortion wave vector (0.5;0.24;0.6) in units of a^*, b^*, and c^* (with a the chain direction). Unlike most charge-density-wave (CDW) materials, the period is commensurate along the chain direction and is incommensurate perpendicular to the chains. The value of $\frac{1}{2}$ is still with respect to the dimerized lattice and is therefore consistent with the $\frac{3}{4}$ band filling previously mentioned. The period measured along the chain direction is also near to the optimum nesting as arrived at by band-structure calculations (Yamaji, 1982, 1983). The existence of an incommensurate SDW has also been established by μSR studies (Le *et al.*, 1991). The magnitude of the magnetic-field distribution, when measured at various temperatures, gives directly the temperature dependence of the order parameter, and experimental results obtained by both NMR and μSR studies are displayed in Fig. 8. The solid line in the figure is the order parameter, obtained from the weak-coupling BCS theory. The somewhat stronger temperature dependence observed experimentally may be due to the fact that the transition to the spin-density-wave ground state is really first order. The

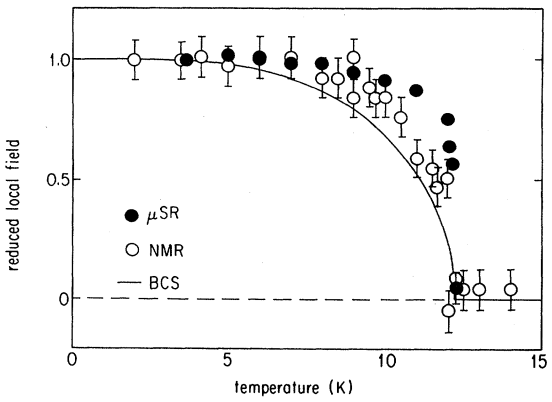

FIG. 8. Temperature dependence of the normalized average internal field at the nuclear sites as measured by nuclear magnetic resonance (NMR) and muon spin rotation (μSR). The bars for the NMR points correspond to a broadening of the resonance due to the incommensurate nature of the SDW (Le *et al.*, 1991; Le *et al.*, 1993).

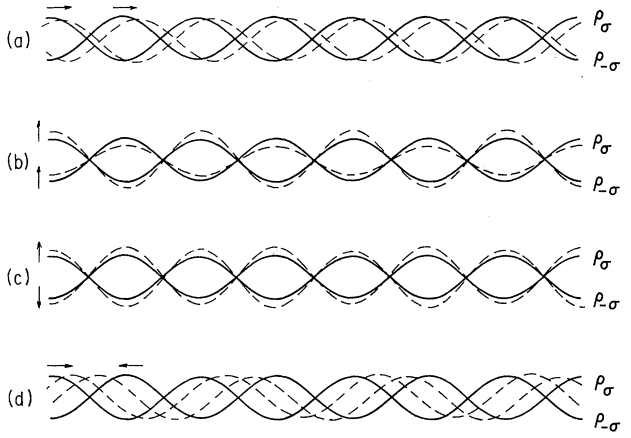

FIG. 9. Various amplitude and phase excitations for a spin-density-wave ground state in the $q=0$ limit. In each case the SDW is viewed as two CDWs—one for each spin subband—with the solid lines (——) indicating the initial state and the dashed lines (— — —) the perturbed state. (a) Both CDWs have been displaced by the same amount in the same direction, leading to a net displacement of the SDW. This is the phason mode. (b) A CDW amplitude excitation in each subband with a phase difference of π between the two is shown. As this would lead to a time-dependent charge density, it is not allowed. (c) Same as in (b), except the excitations are in phase. This excitation is the SDW amplitude mode. (d) Shown is an excitation that modifies the phase difference between the two subbands. Such a distortion leads to a charge buildup and is therefore forbidden.

magnitude of the spin-density-wave modulation can also be extracted from the experimental results, leading to a value of μ/μ_B which is close to that evaluated from NMR studies. This value is in excellent agreement with the magnetic moment evaluated from the measured single-particle gap and Coulomb interaction energy by using Eqs. (3.12), (3.21), and (3.26).

Magnetic susceptibility and NMR studies have also been conducted on $(MDT\text{-}TTF)_2Au(CN)_2$ (Kanoda *et al.*, 1990) and on $(DMET)_2Au(CN)_2$ (Kanoda *et al.*, 1988). In both cases, the magnetic properties are similar to those of an antiferromagnet with a small magnetic moment, and the broadened NMR signal below T_{3D} clearly establishes the incommensurate spin-density-wave ground state. The parameters of the ground state, such as μ/μ_B, have not been evaluated. The development of the SDW ground state also leads to an internal field, shifting the electron-spin-resonance (ESR) frequency up to frequencies determined by the anisotropy factors. Consequently, the conventional ESR signal disappears at T_{SDW}, and this has been observed in the various materials (Walsh *et al.*, 1980; Kanoda *et al.*, 1988, 1990). In addition, spin excitations lead to a relaxation of nuclear spins (Takahashi *et al.*, 1986b). The detailed mechanism is, however, not understood at present.

IV. COLLECTIVE EXCITATIONS

Because of the magnetic character of the spin-density-wave ground state, both spin and charge degrees of freedom are available, and consequently various types of amplitude and phase excitations may occur. With the simple description of the spin-density-wave modulation in the two spin subbands, as given in Fig. 5, these excitations in the long-wavelength limit are shown in Fig. 9. The top part of the figure indicates the displacement of both CDW modulations in the same (say, right) direction, which leads in turn to the displacement of the spin-density-wave modulation. The excitation is analogous to the phase excitations discussed for charge-density waves. The next two parts of the figure describe two different excitations, both related to the change of the amplitudes of the density-wave modulations. The first represents the amplitude fluctuations where the time dependence of the fluctuations is out of phase in the two subbands. This, however, would lead to a time-dependent charge-density-wave component of the order parameter. This would lead to an additional energy and is consequently not allowed. The amplitude fluctuations may also occur in phase, and this leads not to a charge fluctuation but to a change of the amplitude of the spin-density-wave modulation. This excitation corresponds to the amplitude mode as discussed earlier. The fourth possibility, charge-density-wave modulations oscillating in opposite phase, would also lead to a charge-density-wave component, and is thus forbidden.

A. Ginzburg-Landau theory of the excitations

The fluctuations of the amplitude and of the phase of the spin-density-wave modulation are described by the time-dependent Ginzburg-Landau free energy

$$F=n(\varepsilon_F)\left\{a\Delta^2(T)+c\left[\frac{d\Delta}{dx}\right]^2+d\left[\frac{d\Delta}{dt}\right]^2\right\}, \quad (4.1)$$

where the constants a and c can be derived using a microscopic theory. For long-wavelength fluctuations, the order parameter is written as

$$\Delta=(\Delta_0+\delta)e^{i\phi} \quad (4.2)$$

and the oscillations of the magnitude and phase are decoupled. Standard evaluation of the equation of motion leads to two modes, with the dispersion relations (Lee, Rice, and Anderson, 1974; Psaltakis, 1984)

$$\omega_A^2=(2\Delta)^2+(V_Fq)^2 \quad (4.3)$$

for the amplitude mode and

$$\omega_\phi=V_Fq \quad (4.4)$$

for the phase mode at zero temperature and in the $U\rightarrow 0$ limit. These dispersion relations are different from those obtained for charge-density waves (Lee, Rice, and Anderson, 1974). This difference is due to the fact that, in the case of charge-density waves, the charge oscillations are accompanied by ionic motion leading to a significantly enhanced effective mass. No such mass enhancement occurs for spin-density waves. As for charge-density waves, the phase mode is optically active, while the amplitude mode is Raman active.

At finite temperatures, both the amplitude and phase mode have a well-defined temperature dependence. These are determined by the temperature-dependent gap $\Delta(T)$ and by the temperature dependence of the condensate density $f(T)$, which has to be included in Eq. (4.1). Both ω_a and the velocity of the phase mode go to zero at the phase transition and have a characteristic mean-field temperature dependence near $T_{\rm SDW}$.

Coulomb interactions lead to a renormalization of the phason velocity, and the dispersion relation for $U<\varepsilon_F$ is given approximately by

$$\omega_\phi=V_F^0[1+Un(\varepsilon_F)]q\ , \quad (4.5)$$

where V_F^0 here denotes the Fermi velocity in the absence of Coulomb interactions (Psaltakis, 1984).

Next we turn to the spin excitations. In the absence of spin-orbit and dipole-dipole interactions, the spin degrees of freedom have full rotational symmetry. This leads to excitations of a 1D Heisenberg antiferromagnet. These excitations are described by the Hamiltonian (3.37), which accounts well for the static magnetic properties of the SDW ground state. Consequently, results which have been obtained for antiferromagnets can be adapted.

In the absence of magnetic anisotropy fields, the equation of motion

$$\hbar\frac{d}{dt}\langle \mathbf{S}_0\rangle=\mu[\langle \mathbf{S}_0\rangle\times\mathbf{H}_{\rm eff}] \quad (4.6)$$

leads to the dispersion relation

$$\omega=2J_{\rm eff}\lambda q\ . \quad (4.7)$$

The effective coupling constant has been calculated for itinerant electrons. In the weak-coupling limit

$$J_{\rm eff}=\frac{V_F[1-Un(\varepsilon_F)]^{1/2}}{2a}\ , \quad (4.8)$$

while in the strong-coupling limit, $J_{\rm eff}$ is given approximately by (Grüner and Maki, 1991)

$$J_{\rm eff}=\frac{W^2}{4U}\ , \quad (4.9)$$

where W is the bandwidth.

Spin-orbit and dipole-dipole interactions remove the rotational symmetry of the magnetic excitations and lead to an energy gap in the spin-wave excitation spectrum just as for conventional antiferromagnets. The gap and the dispersion relation depend sensitively on the orientation of the external magnetic field with respect to the preferred axis of magnetization. For arbitrary D and E the spin-wave spectrum has two branches, and for zero magnetic field we obtain

$$\hbar\omega_+^2=\frac{\mu}{\mu_B}J_{\rm eff}^2(D+E)\ , \quad (4.10)$$

$$\hbar\omega_-^2=\frac{\mu}{\mu_B}2EJ_{\rm eff}^2\ . \quad (4.11)$$

The magnetic-field dependence of the resonant frequencies can be calculated for various directions of the magnetic field.

B. Collective magnetic excitations of the spin-density-wave state: antiferromagnetic-resonance experiments

The phase and amplitude modes related to charge excitations of the SDW state have not been measured, and neutron- or Raman-scattering studies of these materials have not been performed to date. Optical conductivity measurements, which sample the $q=0$ phase excitations, will be discussed later.

The spin excitations have been examined in various materials through measurements of antiferromagnetic resonance. These experiments add little to our understanding of the SDW state, but give clear evidence that Eq. (3.37) is an appropriate starting point in describing the magnetic properties of the ground state. The experiments are, in general, conducted at fixed measuring frequency, with varying magnetic field and/or temperature. The temperature dependence of the resonance frequency Ω_+ [see Eq. (4.10)] is shown in Fig. 10, together with the magnetic field where the resonance is observed. These values then give, by virtue of Eqs. (4.8) and (4.9), the anisotropy parameters. As expected, D and E are small, because of the small moment μ. A comparison with calculated values gives a rough estimate of $\mu/\mu_B=0.1-0.2$, in good agreement with NMR and μSR studies, discussed earlier.

The thermally induced magnetic excitations also have a profound influence on the temperature dependence of

the magnetization $M(T)$, in a fashion similar to that observed in conventional antiferromagnets. The magnetization is proportional to the internal field, which in turn has been measured to high accuracy by employing muon spin-relaxation experiments (Le *et al.*, 1991), and the results are displayed in Fig. 11. In order to account for the temperature dependence, Eq. (3.37) can be used with the extension from a one-dimensional chain to a system of weakly coupled chains.

For weakly coupled Heisenberg chains, the dispersion relation, keeping only the gap ω_e associated with the larger antiferromagnetic-resonance frequency, is (Kittel, 1963)

$$\omega(k)=\omega_e\{\Delta^2+k_x^2+2\alpha(1-\cos k_y y)\}^{1/2}\ , \qquad (4.12)$$

where $\omega_e=2J_{\rm eff}(\mu/\mu_B)$, $\alpha=J_{\rm eff}/J_\perp$ with $J_\perp$ the perpendicular coupling constant. The gap in the magnon excitation spectrum, given by Eqs. (4.10) and (4.11), is here $\omega_e\Delta$, and we have kept only one gap for the sake of simplicity. Here we have assumed that the dispersion in the third direction can be neglected. The reason for this is the quasi-two-dimensional band structure with the transfer integrals t of the order of 250 meV, 25 meV, and 13 meV, along the chains and in the two directions perpendicular to the chains. As the effective coupling constants in the perpendicular directions are expected to be proportional to t, in the light of the anisotropy of the transfer integrals the 2D limit of the magnon spectrum is justified. (We note that at extremely low temperatures a crossover to a three-dimensional limit occurs. This, however, is expected to arise at temperatures significantly lower than our lowest experimentally accessible temperatures.) The dispersion relation given by Eq. (4.12) has different character at high and at low frequencies, and, depending on the frequency of the magnon modes, two regimes can be distinguished. For $\omega^2-\omega_e^2\Delta^2\gg\alpha\omega_e^2$, $\omega(k)$ is nearly independent of k, and the density of states is that of a 1D magnon spectrum given by

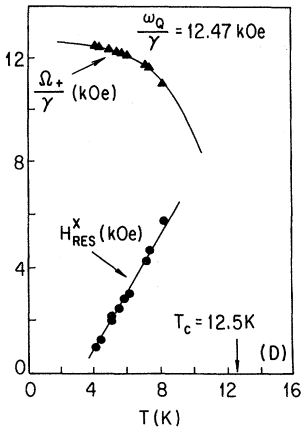

FIG. 10. Antiferromagnetic-resonance frequencies measured along various directions in $(TMTSF)_2AsF_6$. The solid lines are calculated curves based on Eq. (3.37) with the parameters given in the text (Torrance *et al.*, 1982).

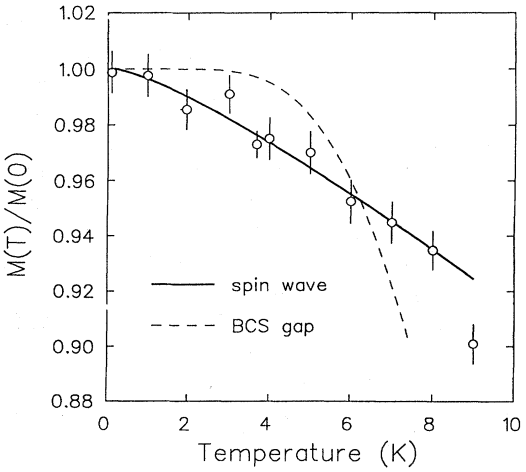

FIG. 11. Comparison of μSR data at low temperatures with model calculations. The solid line shows the 2D spin-wave calculation with an average stiffness constant of 200 K, and the dashed line represents the BCS-gap curve (Lee *et al.*, 1993).

$$\rho(\omega)=\frac{1}{4\pi}\frac{(\omega/\omega_e)^2}{[(\omega/\omega_e)^2-\Delta^2]^{1/2}}\ . \qquad (4.13)$$

for $\omega^2-\omega_e^2\Delta^2\ll\alpha\omega_e^2$, the dispersion relation can be expanded in terms of $k_yJ_\perp$ and

$$\omega(k)=\omega_e\{\Delta^2+k_x^2J_\parallel^2+\alpha k_y^2J_\perp^2\}^{1/2}\ . \qquad (4.14)$$

Consequently, the density of states is

$$\rho(\omega)=\frac{1}{4\pi}\frac{\omega}{\omega_e^2\alpha^{1/2}}\ . \qquad (4.15)$$

An approximate form of the density of states, appropriate for both limits, is given by

$$\rho(\omega)=\frac{1}{4\pi}\frac{\omega/\omega_e^2}{[(\omega/\omega_e^2)-\Delta^2+\alpha]^{1/2}}\ . \qquad (4.16)$$

The magnetization is given, at temperature T, by (Kittel, 1963)

$$M(T)=M_0\int_{\omega_e\Delta}^{\omega_0}\delta\omega\frac{\rho(\omega)}{[(\omega^2/\omega_e^2)-\Delta^2]^{1/2}e^{\omega/kT-1}}\ , \qquad (4.17)$$

with the cutoff frequency defined as

$$\omega_d\int_{\omega_e\Delta}^{\omega_d}\delta\omega\rho(\omega)=\tfrac{1}{2}\ . \qquad (4.18)$$

The magnetization calculated from Eq. (4.17) with the parameters established earlier is displayed in Fig. 11, together with the magnetization as derived from the experiments.

V. IMPURITY EFFECTS

Impurities distributed randomly in the specimens have a profound influence on both the static and dynamic properties of spin-density waves. Impurity potentials that couple directly to the phase ϕ of the condensate des-

troy long-range order (Imry and Ma, 1975; Sham and Patton, 1976) and lead to a finite phase-phase correlation length L_0. The value of L_0 depends on the strength of the impurity potentials, or the impurity concentration, and on the properties of the density wave.

The usual treatment of the problem deals with the impurity effects at low temperatures where amplitude excitations of the collective mode can be neglected; consequently, only the phase degrees of freedom are taken into account. Temperature-induced fluctuations, together with quantum fluctuations of the collective mode, are also neglected. The Hamiltonian that describes the interaction is given within the framework of the Ginzburg-Landau theory (Brazovskii and Dzyaloshinskii, 1976; Fukuyama and Lee, 1978) by

$$H_\phi = \frac{n(\varepsilon_F)V_F^2}{4\Delta^2}\int d\mathbf{r}[(\nabla\phi)^2 + V_{\rm imp}(\phi)] , \tag{5.1}$$

where $(\nabla\phi)^2$ refers to the gradient of the phase, and anisotropy effects due to the anisotropic band structure are neglected. Such effects can be included through the anisotropy of the Fermi velocity V_F. The first term is the usual elastic energy, and the second is the interaction between the collective mode and impurities. As usual, the approach is appropriate for the long-wavelength deformations of the collective mode. Deformations on the length scale $L < \xi_0 = \hbar v_F/2\Delta$ cannot be discussed within the framework of this description.

The mechanism leading to an interaction between charge-density waves and impurities is indicated in Fig. 12(a). The impurity potential $V(\mathbf{k}_i) = V_0\delta(\mathbf{r}-\mathbf{R}_i)$ at $\mathbf{R}_j$ induces a charge-density oscillation with period $\lambda = \pi/k_F$ (the well-known Friedel oscillation), which is phase matched to the density wave. For small impurity potentials, this interaction can simply be written as

$$V_{\rm imp}(\phi) = \int d\mathbf{r}\, V(\mathbf{r}-\mathbf{R}_i)\rho_1\cos[2k_F r + \phi(\mathbf{R}_i)] , \tag{5.2}$$

where ρ_1 is the amplitude of the density-wave modulation in the two spin subbands. Obviously this is appropriate only if the impurity potential does not lead to modification of the amplitude of the collective mode. The amplitude of the spin-density wave is strongly modified near to the impurity if V_0 is comparable to the single-particle gap. The bound impurity states may occur, as discussed in detail by Tütto and Zawadowski (1985; see also Zawadowski and Tütto, 1989).

In the case of spin-density waves, the situation is different. To first order, charged impurities do not interact with the ground state. However, to second order the interaction between the impurity and the two subbands (both with a modulation of the charge density) is different, as indicated in Fig. 12(b), and this leads to an interaction energy given by (Tua and Ruvalds, 1985; Suzumura and Saso, 1987; Tütto and Zawadowski, 1988; Maki and Virosztek, 1989)

$$V_{\rm imp}(\phi) = \int dr\, V(\mathbf{r}-\mathbf{R}_i)\rho_1\cos[4k_F\mathbf{R}_i + 2\phi(R_i)] . \tag{5.3}$$

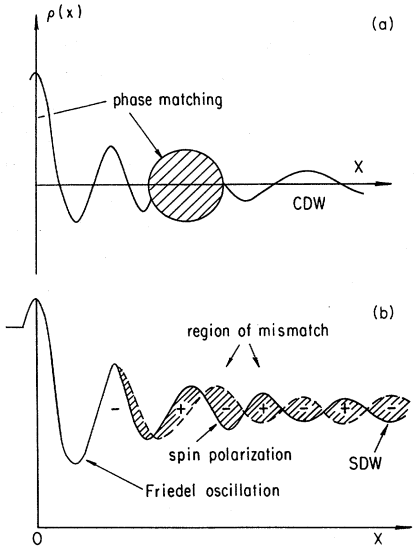

FIG. 12. Spin-density-wave-impurity interaction. (a) Interaction of an electrostatic potential $V(r)$ placed at the origin with a charge-density-wave ground state. The electron density is depicted around an impurity. Between the regions dominated by the Friedel oscillation and the CDW, mismatch regions (hatched) are formed (Zawadowski and Tütto, 1989). (b) Interaction of an electrostatic potential $V(r)$ with a spin-density-wave ground state. The electron densities of up (solid line) and down (dashed line) spin electrons are shown schematically near a nonmagnetic impurity. In the immediate vicinity of the impurity, a charge oscillation known as a Friedel oscillation is formed. Far from the impurity the SDW is not deformed. In the crossover region the mismatch takes place, which is responsible for the pinning (Tütto and Zawadowski, 1988).

In Eq. (5.1) the first term favors a uniform phase, with distortions leading to the increase of the elastic energy. The second term, however, favors local distortions of the phase, thus decreasing the electrostatic interaction energy.

The various situations that may occur have been discussed at length for charge-density waves, and therefore only the main result will be recalled here. For an impurity concentration n_i, the potential-energy gain for a complete adjustment of the density wave at every impurity is given approximately by

$$V_{\rm pot} = V_0\rho_1 . \tag{5.4}$$

This adjustment would, however, lead to an increase of elastic energy, and from Eq. (5.1) this is approximately given by

$$V_{\rm el} = V_F\frac{2\pi}{\langle l\rangle} \simeq V_F n_i , \tag{5.5}$$

where $\langle l\rangle$ is the average distance between the impurities. Consequently, the ratio

$$\varepsilon = \frac{V_{\rm pot}}{V_{\rm el}} = \frac{V_0\rho_1}{V_F n_i} \tag{5.6}$$

tells us whether the impurity–density-wave interaction or the elastic term is more important. The situation where $V_{pot} > V_{el}$ is called strong impurity pinning (the name "pinning" refers to the fact that the collective mode is "pinned" to the underlying lattice through the interaction with impurities).

For $\varepsilon \gg 1$, the potential-energy term dominates, and the total energy of the coupled collective mode and impurity is given by

$$E_{tot} = V_0 \rho_1 n_i \ . \tag{5.7}$$

As the phase is completely adjusted to the impurity positions at every impurity site, the average phase coherence length is given by

$$L_0 \sim \frac{1}{r_i} \ , \tag{5.8}$$

the average distance between impurities.

The case for $\varepsilon \lesssim 1$ is more interesting, and, in this limit, scaling arguments can be used to evaluate the total energy and the phase-phase coherence length (Fukuyama and Lee, 1978; Lee and Rice, 1979). Such arguments lead, in three dimensions, to

$$L_0 = \frac{(\hbar V_F)^2}{(3/2)^2 V_0^2 \rho_1^2 n_i} \ , \tag{5.9}$$

and the characteristic length is inversely proportional to the impurity concentration. From Eq. (5.9) the total-energy gain per unit volume,

$$E_{tot} = \frac{V_0^4 \rho_1^2}{(\hbar V_F)^3} n_i^2 \ , \tag{5.10}$$

is proportional to the square of the impurity concentration.

With a typical impurity potential, $V_0 \simeq 3 \times 10^{-2}$ eV (comparable to the single-particle gap), a Fermi velocity $V_F = 10^7$ cm/sec, and $\rho_1 \sim 10^{-1} \rho_0$, as established from NMR studies (see Sec. III), an impurity concentration of $n_i = 100$ ppm leads to a phase-phase correlation length $L_0 \sim 1\mu$, a macroscopic distance not significantly smaller than the specimen dimensions. This value refers to the length scale of phase correlations along the chain direction. Perpendicular to the chains, the correlation length from Eq. (5.9) is proportional to the square of the anisotropy of the Fermi velocity. For the materials $(TMTSF)_2X$, the anisotropy is of the order of 10 and 250 in the two perpendicular directions; consequently, the coherence length is of the order of 100 Å and 1 Å in the two perpendicular directions. With ξ less than the distance between the chains, arguments based on a three-dimensional anisotropic condensate such as that described by Eq. (5.1) may not apply. This question has, however, not been addressed to date.

The absence of long-range order, as implied by the finite phase-phase correlation length, may have important consequences.

The transition to the SDW state becomes broadened by impurities. In addition, impurities may lead to bound states in the gap (Zawadowski and Tüttő, 1989), which may lead to impurity conduction at low temperatures in a fashion similar to that observed in conventional semiconductors. The finite correlation length is also suggestive of many metastable states, with thermally induced transitions between these states contributing to the low-temperature specific heat in a fashion similar to that observed in charge-density waves (Biljaković *et al.*, 1986).

VI. THE ELECTRODYNAMICS OF SPIN-DENSITY WAVES

Spin-density-wave condensates couple to electromagnetic fields, and the fluctuations of the phase ϕ of the ground state leads to electric current. In the absence of pinning due to impurities and lattice defects, the translational motion of the condensates would lead to a conductivity at zero frequency which, in the absence of damping, would also result in an infinite conductivity. This possibility was first raised by Fröhlich (1954) in connection with charge-density waves. Carrier excitations across the single-particle gap may lead to electromagnetic absorption, with an onset frequency of $\omega_g = 2\Delta/\hbar$ for the absorption process. These features are similar to those observed in superconductors. There are, however, several important differences that lead to electrodynamics fundamentally different from that of the superconducting ground state.

As discussed earlier, the interaction of the collective mode and impurities can, to first order, be represented as a restoring force. This leads therefore to a collective-mode contribution to the conductivity at finite frequency, with $\sigma_{coll} = 0$ at $\omega = 0$. The interaction between the collective modes and lattice vibrations and imperfections leads also to damping and to a finite spectral width of the collective-mode resonances. The dynamics of the internal deformations of the collective modes will, furthermore, lead to long-time or low-frequency relaxational modes, with a frequency-dependent response similar to those observed in glasses and strongly disordered solids.

These aspects are well understood for charge-density waves (Grüner, 1988), where extensive optical experiments clearly identified the single-particle excitations and the contribution of collective-mode resonances. The state of affairs is less clear for spin-density waves, where major disagreement between theory and experiments remains.

A. Models of the frequency-dependent conductivity

As in a superconductor, the phase $\phi(x,t)$ plays an important role in the dynamics of the collective modes for both charge- and spin-density waves. The infinite wavelength phase modes correspond to the translational motion of the condensed electrons. A rigid displacement of the density wave (DW) leads to an electric current, and

the current density per chain is $j_{\rm DW}=-n_c e v_d = -n_{\rm DW} e(d\phi/dt)$. With $\phi=2k_F x$ and $\lambda=\pi/k_F$, we obtain

$$j_{\rm DW}=\frac{e}{\pi}\frac{d\phi}{dt} . \tag{6.1}$$

A compression of the wave leads to a change of the electronic density, and therefore

$$n_c=\frac{e}{\pi}\frac{d\phi}{dx} \tag{6.2}$$

at zero temperature. The cross derivatives of the above equations lead to the equation of continuity,

$$\frac{dj_{\rm DW}}{dx}+\frac{dn_c}{dt}=0 . \tag{6.3}$$

The electric potential couples to the gradient of the phase, and the potential-energy density is given by

$$H_E=\frac{e}{\pi}E\frac{d\phi}{dx} . \tag{6.4}$$

Here the electric field E is applied along the chain direction.

The energy related to the spatial and temporal fluctuations of the phase has been discussed in Sec. IV, and the equation of motion

$$\frac{d\phi^2}{dt^2}-\frac{m}{m^*}V_F^2\frac{d^2\phi}{dx^2}=\frac{2k_F e}{m^*}E(t) \tag{6.5}$$

in the presence of an ac electric field $E(t)=E_0 e^{i(kx-\omega t)}$ leads to

$$\sigma_{\rm coll}(\omega)=\frac{j(\omega)}{E(\omega)}=\frac{m}{m^*}\frac{\omega_p^2}{8}\left[\delta(\omega)+\frac{i2}{\omega\pi}\right] . \tag{6.6}$$

Here m^* is an effective mass associated with the dynamics of the condensate. As discussed in Sec. IV, for spin-density waves, m^* is expected to be the same as the bandmass m_b, and consequently $\omega_p^2=4\pi ne^2/m_b$ is the plasma frequency. The real part,

$$\mathrm{Re}\sigma_{\rm coll}(\omega)=\frac{m}{8m^*}\omega_p^2\delta(\omega) , \tag{6.7}$$

has a Dirac delta singularity at $\omega=0$, with an oscillator strength

$$f=\frac{\pi ne^2}{2m^*} . \tag{6.8}$$

The imaginary part is obtained using the Kramers-Kronig relation,

$$\mathrm{Im}\sigma_{\rm coll}(\omega)=-\frac{2\omega}{\pi}\int_0^\infty\frac{\mathrm{Re}\sigma(\omega')}{\omega'^2-\omega^2}d\omega' = \frac{m}{m^*}\frac{\omega_p^2}{4\pi\omega} . \tag{6.9}$$

The contribution of single-particle excitations is expected, because of the gap, to be similar to that of a semiconductor with a well-defined absorption edge of energy $\hbar\omega=2\Delta$. In the absence of the contribution from the collective mode, the optical conductivity coming from band-to-band transitions is given by

$$\sigma(\omega)=\frac{ne^2}{i\omega m_b}[f(\omega)-f(0)] , \tag{6.10}$$

where, for a one-dimensional electron band,

$$f(\omega)=-f\int dE_k\frac{2\Delta^2/E}{(\omega+i\eta)^2-4E^2} =\frac{2\Delta^2}{\omega y}\left[\pi i+\ln\frac{1-y}{1+y}\right] , \tag{6.11}$$

with $E^2=E_k^2+\Delta^2$, $E_k=\varepsilon_k-\varepsilon_F$, and $y=(1-4\Delta^2/\hbar^2\omega^2)^{1/2}$. Because of the $E^{-1/2}$ singularity of the density of states in one dimension, $\sigma(\omega)$ has a singularity at the gap frequency ω_q. The low-frequency dielectric constant is given by

$$\varepsilon(\omega\to 0)=1-\frac{4\pi}{\omega}\mathrm{Im}\sigma=1+\frac{1}{6}\frac{\hbar^2\omega_p^2}{\Delta^2} , \tag{6.12}$$

where the plasma frequency $\omega_p=(4\pi ne^2/m_b)^{1/2}$.

The relative weight of the collective mode and single-particle contributions to the optical conductivity is determined by sum-rule arguments. The total contribution to the sum rule

$$\frac{2}{\pi}\int[\sigma_{\rm coll}(\omega)+\sigma_{\rm SP}(\omega)]d\omega=\frac{ne^2}{m_b} \tag{6.13}$$

is the same as the sum rule in the metallic state,

$$\frac{2}{\pi}\int\sigma_m(\omega)d\omega=\frac{2}{\pi}\int\frac{ne^2\tau}{m_b(1+\omega^2\tau^2)}d\omega=\frac{ne^2}{m_b} . \tag{6.14}$$

The collective-mode contribution from Eq. (6.8) is

$$I_{\rm coll}=\frac{2}{\pi}\int\sigma_{\rm coll}(\omega)d\omega=\frac{ne^2}{m^*} , \tag{6.15}$$

while the single-particle excitations give a contribution

$$I_{\rm SP}=\frac{2}{\pi}\int\sigma_{\rm SP}(\omega)d\omega=\frac{ne^2}{m_b}-\frac{ne^2}{m^*}=\frac{ne^2}{m_b}\left[1-\frac{m_b}{m^*}\right] . \tag{6.16}$$

For a large effective mass, $m^*/m_b\gg 1$ (as occurs for charge-density waves), nearly all the contribution to the total spectral weight comes from single-particle excitations, while for $m^*/m_b=1$ (the situation appropriate for spin-density waves) all the spectral weight is associated with the collective mode, with no contribution to the optical conductivity from single-particle excitations.

The above arguments are appropriate in the clean limit, $1/\tau\ll\Delta$, which is equivalent to the condition $\xi\ll l$. The response for the opposite case, the so-called dirty limit, $\xi\gg l$, has not been calculated. It is expected, however, that arguments advanced for superconductors apply also for density-wave ground states. As for superconduc-

tors, the collective-mode contribution to the spectral weight is given by the difference

$$\delta=\int[\sigma_m(\omega)-\sigma_{SP}(\omega)]d\omega\ , \tag{6.17}$$

with $\sigma_m(\omega)$ given by Eq. (6.14). This difference is approximately the area given by

$$\int_0^{\omega_g}\sigma_m(\omega)d\omega\simeq 2\sigma_{dc}\Delta=\frac{\omega_p^2}{2\pi^2}\left[\frac{l}{\xi}\right] \tag{6.18}$$

in the dirty limit, with σ_{dc} the dc conductivity. Consequently, the spectral weight due to the mode contribution is reduced with decreasing l/ξ, and an empirical equation, similar to Pippard's equation for the penetration depth (see, for example, Tinkham, 1975), of the form

$$\frac{I^0_{coll}}{I_{coll}}=1+\frac{\xi}{\alpha l} \tag{6.19}$$

can be anticipated. Here I^0_{coll} is the spectral weight of the collective mode in the clean limit. The numerical factor α, however, is expected to be different from unity, which is appropriate for a superconductor.

The collective-mode contribution occurs at zero frequency due to the translational invariance of the ground state. As discussed in Sec. V, in the presence of impurities this translational invariance is broken, and the collective modes are tied to the underlying lattice due to interactions with impurities. To first order this can be described by an average restoring force $k=\omega_0^2 m^*$. Interaction between the collective mode and the lattice imperfections, impurities, etc., may also lead to a finite relaxation time τ^*. With these effects the equation of motion becomes

$$\frac{d^2\phi}{dt^2}+\frac{1}{\tau^*}\frac{d\phi}{dt}+\omega_0^2\phi=\frac{ne}{m^*}E(t)\ , \tag{6.20}$$

leading in the presence of an ac electric field $E(t)=E_0e^{i\omega t}$, to

$$\mathrm{Re}\sigma(\omega)=\frac{ne^2}{m^*}\frac{\omega^2/\tau^*}{(\omega_0^2-\omega^2)^2+(\omega/\tau^*)^2}\ , \tag{6.21a}$$

$$\mathrm{Im}\sigma(\omega)=\frac{ne^2}{m^*}\frac{\omega(\omega_0^2-\omega^2)}{(\omega_0^2-\omega^2)^2+(\omega/\tau^*)^2}\ . \tag{6.21b}$$

For $m^*=m_b$, which is valid for a spin-density ground state, single-particle excitations do not contribute to the optical conductivity in the clean limit, and the collective-mode contribution appears at $\omega=\omega_0$ with

$$\varepsilon(\omega\to 0)=1+\frac{4\pi ne^2}{m_b\omega_0^2} \tag{6.22}$$

having a zero crossing at the plasma frequency $\omega_p=(4\pi ne^2/m_b)^{1/2}$. The response is shown in Fig. 13 with the important parameters also indicated on the figure.

The effect of impurities as described by an average restoring force k is a gross oversimplification: it neglects

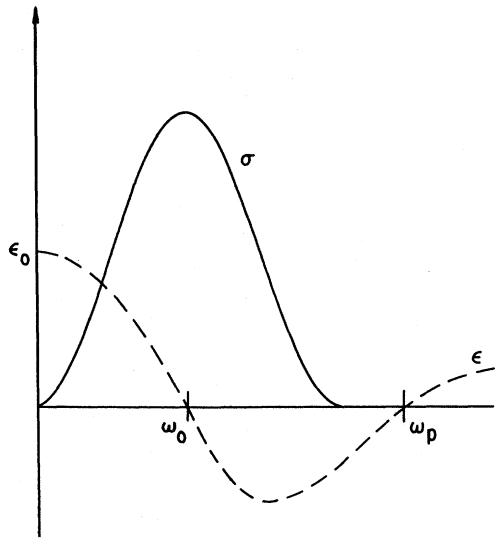

FIG. 13. Frequency dependence of the conductivity and dielectric constant for a spin-density-wave ground state. The figure is appropriate for $\omega_0<\Delta$ and for the clean limit $1/\tau<\Delta$.

the dynamics of the local deformations of the collective modes. The types of process that have been neglected are shown in Fig. 14 for two impurities. The upper part displays an undistorted spin-density wave, with a period $\lambda=\pi/k_F$, and a phase ϕ which is constant. In the presence of impurities, the collective mode is distorted and is adjusted to maximize the energy gain due to interaction with the impurity potential. The resultant distorted density wave is displayed in the middle section of the figure. A low-lying excitation, which involves the dynamics of the internal deformations, is displayed at the bottom of Fig. 14; here a density-wave segment has been displaced by λ, leading to a stretched density wave to the left and to a compressed density wave to the right of the impurity. The local deformation leads to an internal polariza-

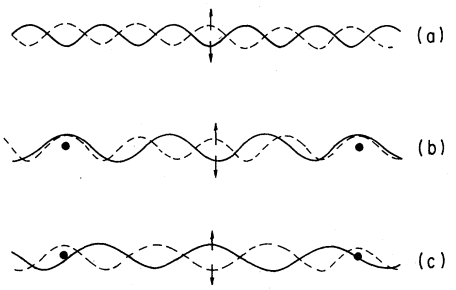

FIG. 14. Following the convention of Fig. 9, with the solid line representing the spin density down, the dashed line the spin-up density-wave distortion: (a) an undistorted spin-density wave. (b) A distortion due to impurities. An expansion of the spin-down-subband allows phase matching at the impurity site. This distortion leads to a charge buildup about the impurity. (c) A low-lying excitation of the spin-density-wave state in which both subbands are stretched in the region between the impurities.

tion by virtue of the displaced charge that accompanies the stretched or compressed density wave. This polarization is given by

$$P(\mathbf{r})=\frac{4\pi c}{\pi}\frac{\partial\phi(\mathbf{r})}{\partial\mathbf{r}} . \tag{6.23}$$

Such processes have been described as a broad superposition of Debye-type processes, and various phenomenological equations have been given to account for the low frequency and long-time behavior of the electrical response. Among these is the so-called Cole-Cole equation,

$$\Sigma(\omega)=\frac{\varepsilon_0}{1+(i\omega\tau_0)^{1-\alpha}} , \tag{6.24}$$

with $\alpha<1$ and τ_0 an average relaxation time. ε_0 is the average dielectric constant frequently used to describe the so-called glassy behavior of a variety of random systems. While these descriptions offer little insight into the microscopic details of the response, they are useful in establishing that it is due to a broad distribution of relaxation times and/or frequencies. They, however, do not address the important issue of fluctuating local electric fields, which arise as the consequences of local deformations of the collective mode. The local deformations, such as those shown in Fig. 14, lead to a spatially inhomogeneous local field $\delta E(k,\omega)$ and also to a current $j(k,\omega)$. The relation between the two quantities is given by

$$\delta j(k,\omega)=\sum_{k'}\sigma(k,k',\omega)\delta E(k',\omega) . \tag{6.25}$$

Because of the local fluctuations of the internal field, the experimentally measured conductivity $\sigma(\omega)$ that relates the spatial averages $\delta E(\omega)$ and $\delta j(\omega)$ through the equation

$$\delta j(\omega)=\sigma(\omega)\delta E(\omega) \tag{6.26}$$

cannot be expressed as $\langle\sigma(k,k',\omega)\rangle=\sigma(k,\omega)\delta_{k,k'}$, and a more sophisticated treatment, which includes the k dependence of the electric-field fluctuations, is required. The issue is complicated, but has received considerable attention recently (Wonneberger, 1991a and references cited therein).

B. Frequency-dependent conductivity of $(TMTSF)_2X$ salts

The frequency-dependent response of spin-density waves is expected to be fundamentally different from the frequency-dependent conductivity observed in the charge-density-wave state. Because the effective mass m^* is the same as the band mass, all the spectral weight is expected to be associated with the collective mode, with single-particle excitations not contributing to $\sigma(\omega)$ in the clean limit. This limit is appropriate in $(TMTSF)_2$ salts, the materials which have been investigated in detail by Walsh *et al.* (1980), Zettl and Grüner (1982a), Jánossy *et al.* (1983), and Javadi *et al.* (1986). The frequency-dependent conductivity measured (Quinlivan *et al.*, 1990; Donovan *et al.*, 1993) in $(TMTSF)_2PF_6$ is shown in Fig. 15 (see also Table IV). The observed behavior is in disagreement with the models of spin-density-wave dynamics discussed earlier. As for charge-density waves, one recovers a resonance in the microwave spectral range, and the most likely explanation is that this resonance is the pinned spin-density-wave mode. The increase of $\sigma(\omega)$ in the far-infrared spectral range is not due to single-particle excitations, as suggested by various groups (Ng *et al.*, 1984; Eldridge and Bates, 1986), since the feature has also been observed above the transition temperature.

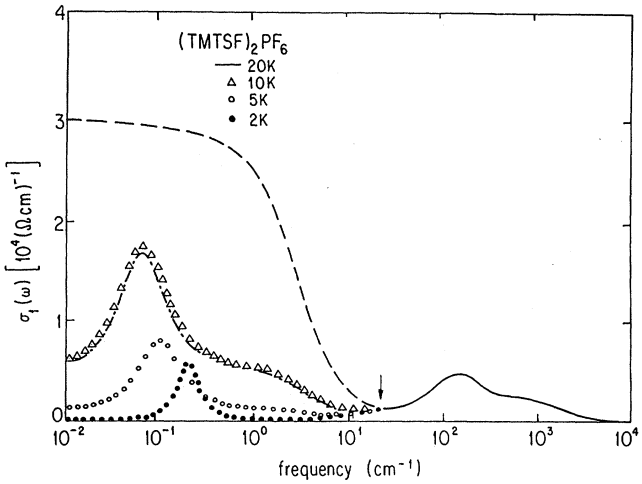

FIG. 15. Frequency dependence of the conductivity measured at various temperatures in $(TMTSF)_2PF_6$. The fit is to Eq. (6.21) with a Drude term due to thermally excited single-particle states (see Table IV). The single-particle gap determined from dc resistivity measurements is indicated by the arrow (Donovan *et al.*, 1993). At each temperature the feature near 100 cm^{-1} was fit with two oscillators ($\nu_{01},\nu_{p1},1/2\pi\tau_1$ and $\nu_{02},\nu_{02},1/2\pi\tau_2$ with $\varepsilon_\infty=2$), while the low-frequency response was modeled with both a Drude ($\nu_p^d,1/2\pi\tau^d$), and a phason ($\nu_0^p,\nu_p^p,1/2\pi\tau^p$) contribution, where the convention $\nu=\omega/2\pi$ was used.

The resonance that occurs at frequencies near

TABLE IV. The parameters (in cm^{-1}) used in the fit to Eq. (6.21).

	ν_{01}	ν_{p1}	$1/2\pi\tau_1$	ν_{02}	ν_{p2}	$1/2\pi\tau_2$	ν_p^d	$1/2\pi\tau^d$	ν_0^p	ν_p^p	$1/2\pi\tau^p$
$T=20$ K:	117	9333	1433	117	5333	200	2500	3			
$T=10$ K:	117	9333	1433	117	5333	200	1050	3	0.067	267	0.1
$T=5$ K:	117	9333	1433	117	5333	200	467	3	0.1	233	0.13
$T=2$ K:	117	9333	1433	117	5333	200	45	3	0.2	217	0.13

$\omega_0/2\pi=3$ GHz has a small and weakly temperature-dependent spectral weight, which is approximately two orders of magnitude smaller than the spectral weight which corresponds to the band mass m_b (Donovan *et al.*, 1992). This gross disagreement between theory and experiment is unaccounted for at present. The small spectral weight could be interpreted as arising because of the large effective mass as seen in Eq. (6.15). The effective mass could be enhanced by the coupling of the spin-density wave to the phonons. This coupling, however, would also lead to a lattice distortion, and this has not been observed (Pouget, private communication). It has also been suggested that long-range Coulomb interactions shift the oscillator strength to the plasma frequency (Maki and Gruner, 1991). This so-called Anderson-Higgs mechanism does not, however, apply to the transverse modes sampled by optical spectroscopy. It is also conceivable that bound states created either by impurities (Zawadowski and Tüttő, 1989) or by discommensurations (Wonnenberger, 1991b) make a large contribution to the spectral weight in the spin-density-wave state. Thus by virtue of the conservation of the total spectral weight the contribution of the pinned mode is small. Further experiments on alloys and on other materials in their SDW state are needed to clarify this point.

The dynamics of the internal deformations of the collective mode have also been examined; and as for charge-density waves, a low-frequency tail develops as the consequence of these deformations. This is shown in Fig. 16 where the conductivity measured (Donovan *et al.*, 1993) in the spin-density-wave state of $(TMTSF)_2PF_6$ is compared with that measured for the charge-density-wave state of $K_{0.3}MoO_3$. Similar behavior has been found by Trætteberg *et al.* (1994). Theories (Littlewood, 1987; Wonneberger, 1991a, 1991b) worked out for the low-frequency dynamics of charge-density-wave states, when extended to account for the spin-density-wave response, are expected to give a good account of the experimental state of affairs. The experimental results obtained on $(TMTSF)_2AsF_6$ are similar (Donovan *et al.*, 1993) to those obtained on the PF_6 salt.

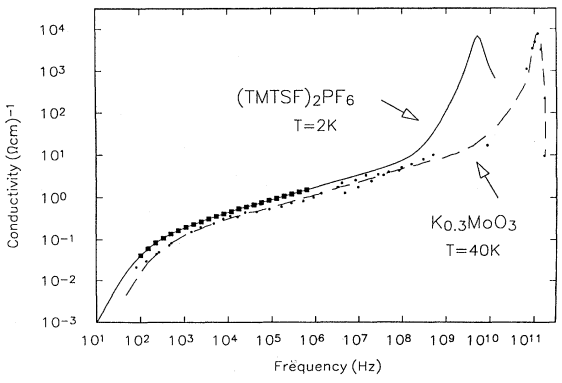

FIG. 16. Frequency dependence of the conductivity of $(TMTSF)_2PF_6$ and $K_{0.3}MoO_3$. The latter compound has a charge-density-wave ground state (Mihály *et al.*, 1991a, 1991b).

In $(TMTSF)_2NO_3$ the collective-mode contribution is not evident, most probably because of the large single-particle contribution to the dc conductivity below T_{SDW} (Donovan *et al.*, 1991).

The temperature dependence of the low-frequency response has also been investigated in detail (Kriza, Kim, *et al.*, 1991). The low-frequency tail, as shown in Fig. 16, progressively freezes out at low temperatures, as expected for internal deformations, the dynamics of which are governed by screening effects due to uncondensed electrons. The long-time behavior of the ac response is given in the time domain by (Mihály and Mihály, 1984)

$$P(t)\approx\exp\left\{-\left[\frac{t}{\tau}\right]^{\alpha}\right\}, \tag{6.27}$$

where the exponent $\alpha\simeq 0.73$ is temperature independent. The average relaxation time $\tau(T)$ has the following temperature dependence,

$$\tau(T)\approx\exp\left[-\frac{\Delta'}{kT}\right], \tag{6.28}$$

where Δ' observed is close to the single-particle gap $\Delta\approx 15$ K. This suggests that the long-time relaxation process is determined by the number of thermally excited single-particle states which screen the internal deformations of the collective mode. These deformations, which can have many possible metastable states close in energy but well separated in space, also lead to hysteresis effects and to memory phenomena. Such effects have been studied extensively for materials with a charge-density-wave ground state (Gill, 1981; Fleming and Schneemeyer, 1983). Memory effects related to the internal deformations of the collective mode have been observed recently in $(TMTSF)_2PF_6$ (Kriza *et al.*, 1992), by driving the collective mode out of equilibrium by the application of electric pulse. During this experiment, pulse sequences, with either the same or opposite polarity for subsequent pulses, are applied, with an amplitude that may exceed the so-called threshold electric field, at which the collective mode is depinned for opposite pulse sequences. The slow discharge is due to the slow relaxation of the collective mode, which approaches equilibrium when the electric field is absent. This excess discharging process has been observed for pulses separated by up to approximately 100 sec, i.e., for time scales orders of magnitude larger than those which characterize the frequency of oscillations of the pinned collective mode. The most likely explanation of the phenomenon is that a reversal of the applied field leads to transitions between different non-equilibrium states, and such states also differ in the macroscopic charge displacement in the specimens. The long-time scales involved then suggest that the relaxational processes which are related to the transitions are extremely slow. This is not unexpected in the light of the very long phase coherence length involved.

VII. NONLINEAR TRANSPORT

The pinned-mode resonance, together with the low-frequency ac response due to the internal deformations of the collective mode, indicates a small overall restoring force k associated with the pinning of the collective mode to the underlying lattice. A small restoring force k is then suggestive of translational motion of the spin-density-wave condensate, which could be induced by a relatively small electric field. The consequence of such motion is a nonlinear current-voltage characteristic. The magnitude of the threshold field for such a translational motion may be estimated as follows: the restoring force ($k = m^* \omega_0^2$) is related to the low-frequency dielectric constant by

$$\varepsilon(\omega \rightarrow 0) = \left[1 + \frac{4\pi n_c e^2}{k} \right] , \tag{7.1}$$

where n_c is the number of electrons per unit volume. The intrinsic periodicity of the SDW is given by λ_0. If the energy $eE\lambda/2$ provided by the applied dc field E over a length $\lambda/2$ is larger than E_{tot}, as given by Eq. (5.10), translational motion of the entire condensate can be induced. Therefore the threshold field is given by

$$E_T = \frac{\lambda k}{2e} , \tag{7.2}$$

which by virtue of Eq. (7.1) can also be written as

$$E_T \varepsilon(\omega \rightarrow 0) = 4\pi e n_\perp \tag{7.3}$$

where $n_\perp$ is the number of chains per unit cross section. The above arguments neglect the role played by internal deformations which modify both $\varepsilon(\omega \rightarrow 0)$ and the threshold field E_T. However, Eq. (7.3) was found to be approximately obeyed for a variety of compounds with a charge-density-wave ground state, for which similar arguments apply (Wu *et al.*, 1984; Grüner, 1988).

Although early observations on nonlinear transport in the SDW state were thought to be due to spurious effects, nonlinear transport with a well-defined threshold field has now been found in a variety of compounds with a SDW ground state. This finding, together with various other experiments discussed later, directly confirms the translational motion of the condensate. Furthermore, at low temperatures a novel type of transport, different from those observed at high temperatures (and in compounds with a CDW ground state), has been found.

A. Nonlinear spin-density-wave conduction

Early experiments on $(TMTSF)_2PF_6$, while clearly showing nonlinear conductivity in the spin-density-wave state (Walsh *et al.*, 1980; Chaikin *et al.*, 1980, 1981), did not give evidence for a sharp threshold field for the onset of nonlinear conduction, like that observed for charge-density waves. Consequently, the nonlinear response was thought to arise as the consequence of hot-electron effects, which occur because of the long mean free path in these materials. Clear evidence for a sharp threshold field was observed significantly later: $(TMTSF)_2NO_3$ (Tomić *et al.*, 1989); $(TMTSF)_2PF_6$ (Kang *et al.*, 1990); and $(TMTSF)_2ClO_4$ (Sambongi *et al.*, 1989). The nonlinear characteristics observed in the $(TMTSF)_2ClO_4$ are displayed in Fig. 17, while in Fig. 18 the differential resistance is displayed for $(TMTSF)_2AsF_6$ as a function of electric field (Tomić *et al.*, 1991).

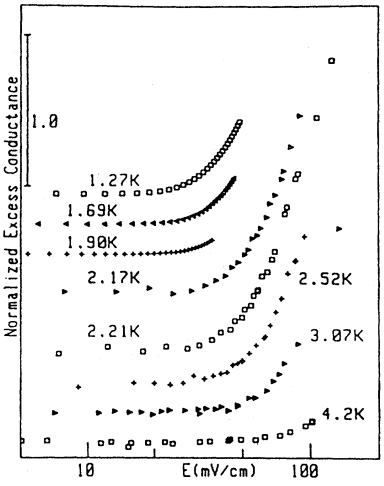

FIG. 17. Field dependence of the conductance at various temperatures on the SDW state of $(TMTSF)_2ClO_4$ (Sambongi *et al.*, 1989).

The behavior shown in Figs. 17 and 18 is characteristic of the nonlinear behavior of the resistivity seen in several materials with a CDW ground state (Grüner, 1988). The well-defined threshold field, and the smooth rise of the conductivity, with no divergence in the differential conductivity, has been interpreted (see, for example, Gor'kov and Grüner, 1989) as evidence for the important role played by the internal deformations of the collective mode. Several models account for the smooth onset of nonlinearity, all based on mechanisms in which the internal mode dynamics are significant. Further evidence for

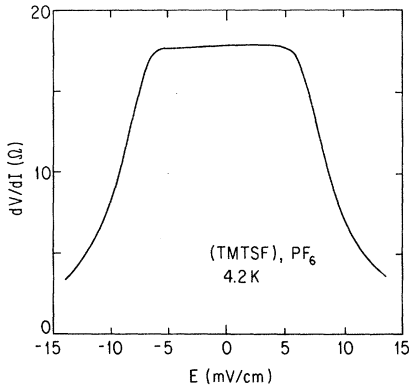

FIG. 18. Differential resistance measured as a function of electric field E in the spin-density-wave state of $(TMTSF)_2PF_6$ (Tomić *et al.*, 1991).

this comes from experiments where both E_T and ε ($\omega \to 0$) are measured and the two experimentally observed quantities are connected to each other. As discussed earlier, E_T and ε ($\omega \to 0$) are related through the relation (7.3), which also describes approximately the behavior in a variety of materials with a CDW ground state. In Fig. 19, this connection is shown for various compounds, in all cases in the limit where internal deformations of the collective modes are important (Grüner, 1988). Based on the above considerations, it is expected that models originally worked out for CDW dynamics will have the same success (or limitations) in describing the dynamics of spin-density waves.

Because of the dynamics of internal deformations, which are screened by normal electrons, it is expected that the nonlinear conduction is influenced also by screening effects. If screening by uncondensed electrons is important, and they determine the damping of the collective mode, the nonlinear response is proportional to the Ohmic conductivity as first shown by Fleming *et al.* for charge-density waves in 1986. This has also been observed (Chaikin *et al.*, 1981; Kriza, Quirion, Trætteberg,and Jérome, 1991) in $(TMTSF)_2PF_6$, where the Ohmic conductivity σ_{Ohmic} was changed by varying the temperature or by applying an external magnetic field. This close correspondence between the Ohmic and nonlinear part of the conduction process has been accounted for by Sneddon (1984) and, in more detail, by Littlewood (1987), who showed that in the case of the dynamics of internal deformations, the damping arises due to quasiparticle screening currents.

The temperature dependence of the threshold field E_T has also been investigated in detail (Shimizu *et al.*, 1991; Tomić *et al.*, 1991) in $(TMTSF)_2ClO_4$ and in the PF_6 salts of TMTSF. In both cases the threshold field slowly decreases with decreasing temperature. The behavior has been accounted for (Maki and Virosztek, 1990a, 1990b) by a model where the internal deformations of the condensate are neglected. Consequently, this model most probably has no direct relevance to the experimental findings.

Direct evidence that the pinning, and consequently the threshold field E_T, is determined by impurities comes from studies where such impurities are introduced either by irradiation (Kang *et al.*, 1991; Tomić *et al.*, 1991) or by alloying (Trætteberg *et al.*, 1994). In the former case it was found that E_T is proportional to the impurity concentration, and therefore it appears that defects created by irradiation act as strong pinning centers. Experiments in a series of alloys in which a fraction of the As atoms are substituted by Sb are displayed in Fig. 20. By assuming a residual impurity concentration x_0 for the nominally pure specimen of $(TMTSF)_2AsF_6$, the behavior can be described, as indicated by the solid line in Fig. 20, by the relation

$$E_T(x)=E_2(x=0)+Ax^2\ ; \tag{7.4}$$

and, consequently, it appears that, upon alloying, weak impurity pinning occurs as described in the previous section.

In some cases the depinning of charge-density waves is abrupt and is accompanied by hysteresis effects (Zettl and Grüner, 1982a, 1982b). This behavior is most probably associated with extended defects, such as grain boundaries, and with the collapse of the order parameter at these extended defects. Similar behavior has been observed in some cases in materials with a SDW ground state; a typical example is displayed in Fig. 21. The behavior may also be due to the presence of macroscopic defects, such as grain boundaries, in the specimens.

The magnitude of the nonlinear conductivity also depends strongly on the impurity concentration

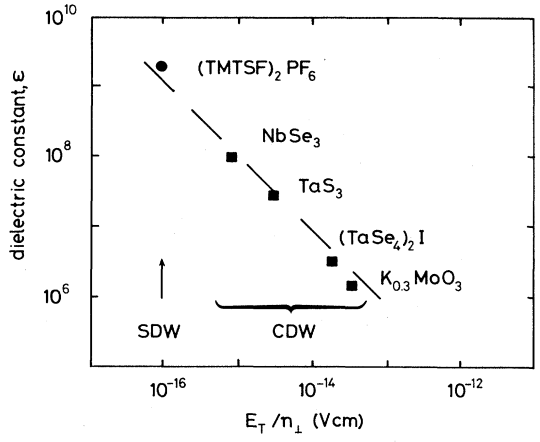

FIG. 19. Low-frequency dielectric constant vs the threshold field (normalized to one chain) for $(TMTSF)_2PF_6$ and for various materials with a CDW ground state (Mihály *et al.*, 1991a). $n_\perp$ is the number of conducting chains per unit cross section. The dashed line is a plot of $E_T\varepsilon(\omega \to 0)=en_\perp$.

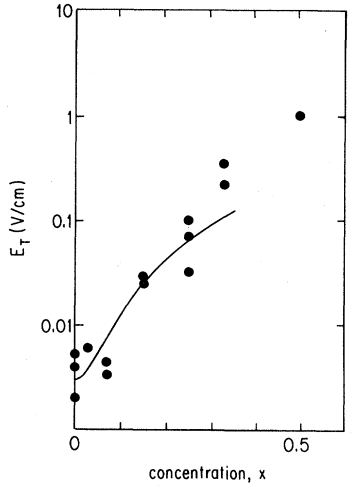

FIG. 20. Threshold field E_T as the function of alloying concentration in $(TMTSF)_2(AsF_6)_{1-x}$ alloys. The solid line is Trætteberg *et al.* (1994), a fit to $E_T(x)=E_T(x=0)+Ax^2$ with $A \simeq 1$ V/cm.

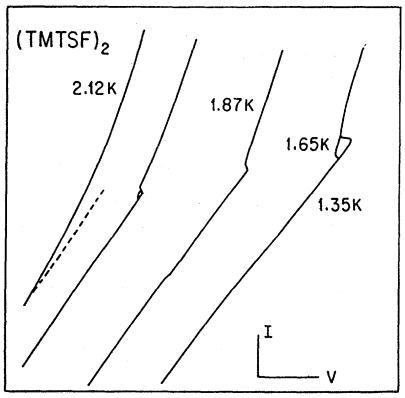

FIG. 21. Current-voltage characteristics observed in $(TMTSF)_2ClO_4$ (Sambongi *et al.*, 1989). The hysteresis near the threshold field is clearly visible.

(Trætteberg *et al.*, 1994), particularly at temperatures close to the transition. The behavior is displayed in Fig. 22. This suggests that the damping, which is related to the moving condensate, is strongly concentration dependent, in a fashion similar to Matthiessen's rule in normal metals. It has been suggested that the concentration-dependent damping (which is also temperature independent) arises as the consequence of the elastic scattering of phasons by defects. The same applies to the low-frequency conduction. This has also been shown by Trætteberg *et al.* (1993).

The relation between the frequency-dependent and nonlinear conductivity, expressed by Eq. (7.3), has also been established in pure $(TMTSF)_2PF_6$ (Mihály *et al.*, 1991a) and on alloys (Trætteberg *et al.*, 1994).

B. Current oscillations and interference effects

The periodicity of the SDW condensate is related to some fundamental periodicity associated with the translational motion. A drift velocity v_d leads to a time-average current, $j_{SDW}=n_c e v_d$, while the fundamental frequency associated with a displacement of the collective mode through one period is $f_0=v_d/\lambda_0$. Therefore

$$\frac{j_{SDW}}{f_0}=n_c e\lambda_0 \; ; \tag{7.5}$$

and since $n_c=2k_F/\pi$ and $\lambda_0=\pi/k_F$, thus

$$\frac{j_{SDW}}{f_0}=2e \; . \tag{7.6}$$

Such oscillations have been observed directly in $(TMTSF)_2ClO_4$ (Nomura *et al.*, 1989; Hino *et al.*, 1991), and the latter observations are displayed in Fig. 23. A fundamental and a first harmonic (with both frequencies increasing with the current carried by the condensate) are observed, together with several minor peaks in the Fourier-transformed current spectrum. Both observations, while clearly establishing the intrinsic current oscillation phenomena, also point to inhomogeneous current distribution in the specimens. This may arise as a consequence of the high anisotropy, but may also be due to breaks that may develop during the cooldown process.

The intrinsic frequency f_0 (and its harmonics) can also be explored by applying both dc and ac electric fields, with the total driving force

$$E=E_{dc}+E_{ac}\cos\omega_{ext}t \; . \tag{7.7}$$

When f_0 (or its harmonics) coincides with $\omega_{ext}/2\pi$ (or with its harmonics), interference effects occur, and they

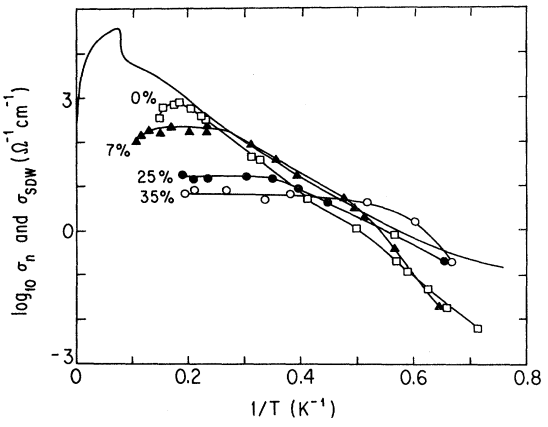

FIG. 22. Nonlinear conductivity, measured at $E=2E_T$ for various concentrations in $(TMTSF)_2(AsF_6)_{1-x}(SbF_6)_x$ alloy together with the Ohmic conductivity (solid line). (Trætteberg *et al.*)

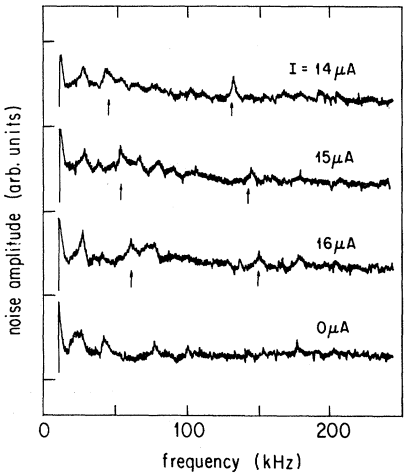

FIG. 23. "Noise" amplitude observed by using a spectrum analyzer for different currents in a sample of $(TMTSF)_2ClO_4$. The arrows refer to the fundamental and to the first harmonic of the oscillation frequency (Hino *et al.*, 1991).

influence the dc current-voltage characteristics. Early observations of this kind made on charge-density waves have been accounted for by a model where the internal degrees of freedom of the condensate are neglected and the equation of motion of the collective coordinate is described as (Grüner *et al.*, 1981)

$$\frac{dx^2}{dt^2}+\Gamma\frac{dx}{dt}+\omega_0^2 x = E_{dc}+E_{ac}e^{i\omega_{ext}t} . \tag{7.8}$$

The equation of motion is formally identical to the equation describing the resistively shunted Josephson junction; consequently, the interference features are referred to as "Shapiro steps" (Shapiro, 1963; Zettl and Grüner, 1984). Such Shapiro steps have been observed in $(TMTSF)_2PF_6$, and the experimental findings are shown in Fig. 24. Both harmonic and subharmonic Shapiro steps have been observed, which give clear evidence for nonsinusoidal oscillations and for the importance of internal degrees of freedom (Kriza, Quirion, Trætteberg, Kang, and Jérome, 1991). Such studies also establish the current dependence of the fundamental frequency and a linear relation,

$$I_{SDW}=\text{const}\times f_0 . \tag{7.9}$$

This relation, both for the fundamental frequency f_0 and for the first harmonic and the subharmonic, corresponding to $\frac{1}{2}f_0$, is displayed in Fig. 25. The linear relation is in full agreement with Eq. (7.5). The constant that relates the current density to the fundamental frequency is different from the value $2e$ given by Eq. (7.6), and the available experimental results indicate a current that is significantly smaller than that corresponding to Eq. (7.6).

Several explanations have been advanced to account for this discrepancy. One likely explanation is that the difference is due to the highly anisotropic nature of the conduction process, which leads to current only at the surface of the material, where the voltage and current probes are applied. Estimates of the effective area (based on the Ohmic conductance) lead to experimental results in broad agreement with Eq. (7.6).

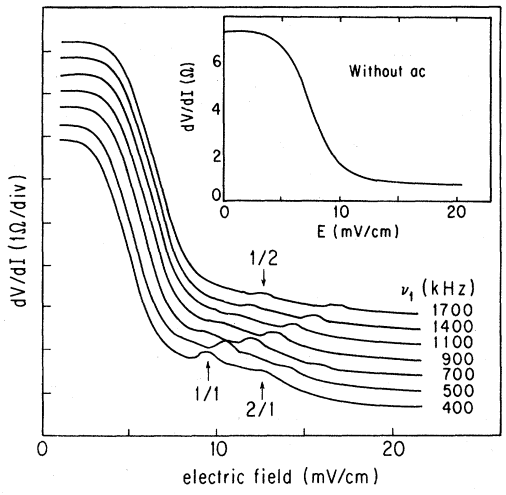

FIG. 24. Differential resistance observed in $(TMTSF)_2AsF_6$ in the presence of an ac electric field of frequency ν. The arrows show the interference peaks for the fundamental, first harmonic, and first subharmonic frequency (Kriza, Quirion, Trætteberg, Kang, and Jérome, 1991). The inset shows the differential resistance in the absence of an ac field.

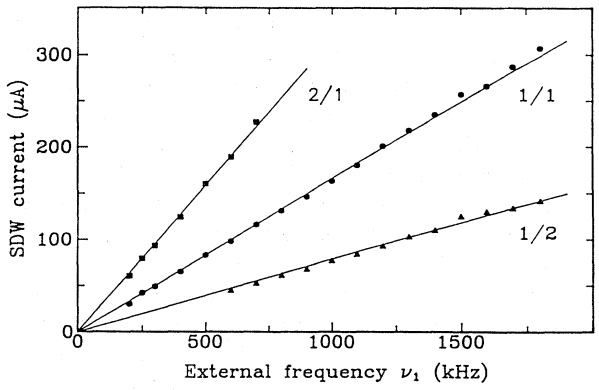

FIG. 25. Frequency of the fundamental oscillation frequency (1/1), the second harmonic (2/1), and the first subharmonic (1/2) vs the excess current carried by the spin-density wave (Kriza, Quirion, Trætteberg, Kang, and Jérome, 1991).

C. Properties other than electrical conduction

The onset of nonlinear conduction, which leads to nonlinear current-voltage characteristics, is also accompanied by various anomalies. The development of the SDW ground state and the development of a gap in the single-particle excitation spectrum lead to a stiffening of the underlying lattice and to an anomaly in the elastic damping constant. Upon application of an electric field E that exceeds E_T, the lattice becomes progressively softer, and there is an associated increase of the damping constant (Brown *et al.*, 1992). Both effects are similar to the observations made on charge-density waves (Brill and Roark, 1984; Mozurkewich *et al.*, 1985). Several models have been proposed to account for the experimental findings made on charge-density waves, and they may also be appropriate for spin-density-wave dynamics. While the details of the mechanism leading to changes in the elastic properties remain unresolved, it is clear that the spin-density-wave ground state couples to the underlying lattice through impurities and other lattice defects; and this coupling is primarily responsible for the anomalies observed in the compound $(TMTSF)_2PF_6$.

The development of the incommensurate spin-density-wave modulation also leads to a broadening of the NMR line measured on H^1 nuclei. This broadening, shown in Fig. 8, arises as a consequence of the distribution of the internal magnetic field at the nuclear sites, and a detailed analysis of the line shape directly gives the wave vector Q

of the spin-density-wave modulation. When the ground state executes a translational motion, the internal field at the nuclear sites fluctuates in time; and for a fast enough fluctuation (when compared with the nuclear Larmor frequency), motional narrowing may occur. While the first observations (Delrieu and Kinoshita, 1992) might be influenced by heating, the effect, which is regarded as clear evidence for the translational motion of the spin-density-wave ground state, has been observed in $(TMTSF)_2PF_6$ (Barthel *et al.*, 1993; Wong *et al.*, 1993). Both groups have eliminated the possibility of heating by measuring the Knight shift (which was found to be different from the Knight shift in the metallic state) and by measuring the nuclear-spin temperature (and consequently the temperature of the specimens) directly. A detailed analysis that would allow the evaluation of the drift velocity has not been performed, to date.

D. Nonlinear effects at low temperatures

The observations made on $(TMTSF)_2X$ salts at temperatures not far below their transition temperatures have all the hallmarks of a depinning process, where the internal degrees of the condensate play an important role. Furthermore, the existence of the well-defined threshold field and long-time relaxational phenomena is usually interpreted within the framework of models where classical equations of motion, without tunneling steps, govern the dynamics of the condensate (Littlewood, 1987 and references cited therein). Upon decreasing the temperature, this type of nonlinear transport process progressively freezes out, and a qualitatively different nonlinear current-voltage characteristic is observed (Mihály *et al.*, 1991b). The crossover between the high- and low-temperature nonlinear transport is shown in Fig. 26. At temperatures above approximately 1.5 K, a well-defined threshold, shown by the arrow labeled E_T, is observed. This behavior progressively disappears with decreasing temperature, and below about 1 K a different type of nonlinearity occurs. In this temperature range the nonlinear conduction is independent of the temperature and can be described well, over a broad electric-field range, by

$$\sigma=\sigma_0 e^{-E_0/E} . \tag{7.10}$$

The functional form of $\sigma(E)$ and also the temperature-independent response are suggestive of a current determined by a tunneling process, and indeed Eq. (7.10) is identical to the expression that describes single-particle Zener tunneling across the spin-density-wave gap. For Zener tunneling the characteristic field E_0 is given by

$$E_0=\frac{\pi^2}{4}\frac{\Delta^2}{Dea} , \tag{7.11}$$

where D is the bandwidth and a is the lattice constant. The single-particle gap $\Delta=15$ K, together with the single-particle bandwidth $D\simeq 1$ eV (Jérome and Schultz, 1982), leads to $E_0=1.1\times 10^3$ eV, approximately three orders of magnitude larger than the value of $E_0=3$ V/cm obtained by fitting the experimental data to Eq. (7.10). Studies on both $(TMTSF)_2PF_6$ and $(TMTSF)_2AsF_6$ and their alloys indicate that E_0 increases nearly linearly with increasing impurity concentration, but the precise functional dependence of E_0 on n_i has not yet been established (Kim *et al.*, 1993; Trætteberg *et al.*, 1994). The low-temperature response has also been examined as a function of external magnetic field and pressure (Trætteberg *et al.*, 1992; Kim *et al.*, 1993). The magnetic field does not modify E_0, but σ_0 has a field dependence that is similar to $\sigma(H)$ observed for the Ohmic conductivity due to thermally excited carriers (Chaikin *et al.*, 1982). This would then suggest that the carriers created by the tunneling process are identical to the thermally excited carriers. The applied pressure leads to a decrease of the single-particle gap and of E_0, and one finds that, approximately, $E_0\sim\Delta^2$. Such behavior follows from any model where the tunneling barrier is proportional to the single-particle gap.

It is not clear at present what type of tunneling leads to the observed nonlinear conduction at low temperatures. It has been suggested that tunneling due to solitons which arise as the consequence of commensurability or near commensurability takes place (Wonneberger, 1991b), but the impurity dependence of E_0 appears to rule this out. The small observed value of E_0 also rules out simple Zener tunneling, while tunneling that involves impurity states in the gap would not lead to a concentration-dependent characteristic field.

Further experiments, possibly involving the joint application of dc and ac excitations, are required to clarify the nature of this remarkable phenomenon.

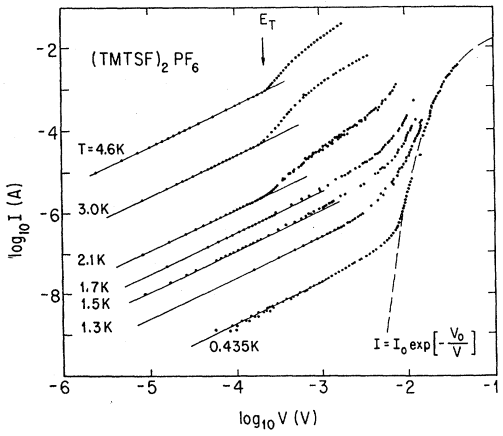

FIG. 26. Current-voltage characteristics measured in $(TMTSF)_2PF_6$ at various temperatures. At high temperatures a sharp onset of nonlinear conduction can be clearly seen. However, at the lowest temperatures, this sharp threshold is no longer visible; rather, a smooth onset occurs to a tunneling type of behavior (Mihály *et al.*, 1991b).

VIII. CONCLUSIONS

The existence of a spin-density-wave ground state is by now firmly established in various organic linear-chain compounds through a variety of transport and magnetic studies. Because of the large anisotropy, the Fermi surface is entirely removed by the transition to the spin-density-wave state, and the ground state is close to that of an antiferromagnet described by phenomeonological parameters such as the exchange constant J_{eff} and magnetic moment μ. The large magnetic coupling and small magnetic moment are in agreement with a spin-density wave in the weak-coupling limit.

Because of the magnetic character of the ground state, and because of the charge modulations in the two spin subbands, both spin and charge excitations occur; and the magnon and phason dispersion relations are well understood. In the long-wavelength limit, these have been explored by antiferromagnetic resonance and by ac conductivity measurements. While the magnon excitations are well understood, the phason excitations have a spectral weight significantly smaller than expected. The reason for this is not understood, and other resonances associated with the SDW ground state may account for the missing spectral weight.

Many of the observations on nonlinear transport are reminiscent of the nonlinear response of charge-density waves, and models applied to the latter are expected to account for the experimental findings summarized here. The new type of transport that occurs at low temperatures, and which is suggestive of tunneling effects, has not been explained to date and remains one of the major unresolved issues of the field.

One should also stress that the observations on the dynamics have been made on $(TMTSF)_2X$ salts, and attempts to observe the dynamics of spin-density waves in other materials with a well-defined SDW ground state, discussed in Sec. III, were not successful. Clearly, further experiments are required before the universal features of the dynamics of this new type of collective mode are clearly established.

ACKNOWLEDGMENTS

I gratefully acknowledge discussions with Stuart Brown, Tamas Csiba, Steve Donovan, Yong Kim, Tomo Uemura, and Attila Virosztek. Several comments by Dennis Jérome, George Kriza, and Ola Trætteberg were also most helpful, and the permission to use their experimental results are also gratefully acknowledged.

Many of the results described in this review were obtained with the help of NSF Grant DMR-89-13236.

REFERENCES

Andrieux, A., D. Jérome, and K. Bechgaard, 1981, J. Phys. Lett. **42**, L87.

Barthel, E., G. Kriza, G. Quirion, P. Wzietek, D. Jérome, J. B. Christensen, M. Jørgensen, and K. Bechgaard, Phys. Rev. Lett. **71**, 2825 (1993).

Bechgaard, K., C. S. Jacobsen, K. Mortensen, H. J. Pedersen, and N. Thorup, 1980, Solid State Commun. **33**, 1119.

Biljaković, K., J. C. Lasjaunias, F. Zougmore, P. Monceau, F. Levy, L. Bernard, and R. Currat, 1986, Phys. Rev. Lett. **57**, 1907.

Brazovskiĭ, S. A., and I. E. Dzyaloshinskiĭ, 1976, Zh. Eksp. Teor. Fiz. **71**, 2338 [Sov. Phys. JETP **44**, 1233 (1976)].

Brill, J. W., and W. Roark, 1984, Phys. Rev. Lett. **53**, 846.

Brown, S. E., B. Alavi, G. Grüner, and K. Bartholomew, 1992, Phys. Rev. B **46**, 10483.

Chaikin, P. M., G. Grüner, E. M. Engler, and R. L. Greene, 1980, Phys. Rev. Lett. **45**, 1874.

Chaikin, P. M., P. Haen, E. M. Engler, and R. L. Green, 1981, Phys. Rev. B **24**, 7155.

Creuzet, F., T. Takahashi, D. Jérome, and J. M. Fabre, 1982, J. Phys. (Paris) Lett. **43**, L755.

Delrieu, J. M., and N. Kinoshita, 1992, Synth. Met. **41-43**, 3947.

Delrieu, J. M., M.Roger, Z. Toffano, A. Moradpour, and K. Bechgaard, 1986, J. Phys. **47**, 839.

Delrieu, J. M., M. Roger, Z. Toffano, E. Wope Mbougue, P. Fauvel, R. Saint James, and K. Bechgaard, 1986, Physica B **143**, 412.

Donovan, S., L. Degiorgi, and G. Grüner, 1992, Europhys. Lett. **19**, 433.

Donovan, S., K. Holczer, and G. Grüner, 1991, Synth. Met. **41**, 3877.

Donovan, S., K. Holczer, G. Grüner, K. Maki, and F. Wudl, 1993, unpublished.

Eldridge, J., and G. S. Bates, 1986, Phys. Rev. B **34**, 6992.

Fleming, R. M., R. J. Cava, L. F. Schneemeyer, E. A. Rietman, and R. G. Dunn, 1986, Phys. Rev. B **33**, 5450.

Fleming, R. M., and L. F. Schneemeyer, 1983, Phys. Rev. B **28**, 6996.

Fröhlich, H., 1954, Proc. R. Soc. London Ser. A **223**, 296.

Fukuyama, H., and P. A. Lee, 1978, Phys. Rev. B **17**, 535.

Gill, J. C., 1981, Solid State Commun. **39**, 1203.

Gor'kov, L. P., and G. Grüner, 1989, Eds., "Charge Density Waves in Solids" in *Modern Problems in Condensed Matter Sciences, Vol. 25* (North-Holland, Amsterdam).

Grüner, G., 1988, Rev. Mod. Phys. **60**, 1129.

Grüner, G., and K. Maki, 1991, Comments Condens. Matter Phys. **15**, 145.

Grüner, G., A. Zawadowski, and P. M. Chaikin, 1981, Phys. Rev. Lett. **66**, 3641.

Hino, N., T. Sambongi, K. Nomura, M. Nagasawa, M. Tokumoto, H. Anzai, N. Kinoshita, and G. Saito, 1991, Synth. Met. **40**, 275.

Honda, Y., K. Murata, K. Kikuchi, K. Saito, I. Ikemoto, and K. Kobayashi, 1989, Solid State Commun. **71**, 1087.

Huang, X., and K. Maki, 1990, Phys. Rev. B **42**, 6498.

Imry, Y., and S. K. Ma, 1975, Phys. Rev. Lett. **35**, 1399.

Jacobsen, C. S., D. B. Tanner, and K. Bechgaard, 1982, Mol. Cryst. Liq. Cryst. **79**, 25.

Jacobsen, C. S., D. B. Tanner, and K. Bechgaard, 1983, Phys. Rev. B **28**, 7019.

Jánossy, A., M. Hardiman, and G. Grüner, 1983, Solid State Commun. **46**, 21.

Javadi, H., S. Sridhar, G. Grüner, L. Chiang, and F. Wudl, 1986, Phys. Rev. Lett. **55**, 1216.

Jérome, D., and H. Schultz, 1982, Adv. Phys. **32**, 299.

Kang, W., S. Tomić, J. R. Cooper, and D. Jérome, 1990, Phys. Rev. B. **41**, 4862.

Kang, W., S. Tomić, and D. Jérome, 1991, Phys. Rev. B **43**, 1264.
Kanoda, K., Y. Kobayashi, T. Takahashi, T. Inukai, and G. Saito, 1990, Phys. Rev. B **42**, 8678.
Kanoda, K., T. Takahashi, T. Tokiwa, K. Kikuchi, K. Saito, I. Ikemoto, and K. Kobayashi, 1988, Phys. Rev. B **38**, 39.
Kikuchi, K., K. Murata, M. Kikuchi, Y. Honda, T. Takahashi, T. Oyama, I. Ikemoto, T. Ishiguro, and K. Kobayashi, 1987, Jpn. J. Appl. Phys. **26**, Suppl. **26-3**, 1369.
Kim, Y., S. Donovan, and G. Grüner, 1993, unpublished.
Kittel, C., 1963, *Quantum Theory of Solids* (Wiley, New York).
Kriza, G., Y. Kim, A. Beleznay, and G. Mihály, 1991, Solid State Commun. **71**, 811.
Kriza, G., Y. Kim, and G. Mihály, 1992, Phys Rev. B **45**, 466.
Kriza, G., G. Quirion, O. Trætteberg, and D. Jérome, 1991, Europhys. Lett. **16**, 585.
Kriza, G., G. Quirion, O. Trætteberg, W. Kang, and D. Jérome, 1991, Phys. Rev. Lett. **66**, 1922.
Le, L. P., G. M. Luke, B. J. Sternlieb, W. D. Wu, Y. J. Uemura, J. H. Brewer, T. M. Riseman, R. V. Upasani, L. Y. Chiang, and P. M. Chaikin, 1991, Europhys. Lett. **15**, 547.
Le, L. P., *et al.*, 1993, Phys. Rev. B **48**, 7289.
Lee, P. A., and T. M. Rice, 1979, Phys. Rev. B **19**, 3970.
Lee, P. A., T. M. Rice, and P. W. Anderson, 1974, Solid State Commun. **14**, 703.
Littlewood, P., 1987, Phys. Rev. B **36**, 3108.
Maki, K., and G. Grüner, 1991, Phys. Rev. Lett. **66**, 782.
Maki, K., and A. Virosztek, 1989, Phys. Rev. B **39**, 9640.
Maki, K., and A. Virosztek, 1990a, Phys. Rev. B **41**, 557.
Maki, K., and A. Virosztek, 1990b, Phys. Rev. B **42**, 655.
Mihály, G., Y. Kim, and G. Grüner, 1991a, Phys. Rev. Lett. **66**, 2806.
Mihály, G., Y. Kim, and G. Grüner, 1991b, Phys. Rev. Lett. **67**, 2713.
Mihály, G., and L. Mihály, 1983, Solid State Commun. **48**, 449.
Mihály, G., and L. Mihály, 1984, Phys. Rev. Lett. **52**, 149.
Mortensen, K., Y. Tomkiewicz, and K. Bechgaard, 1982, Phys. Rev. B **25**, 3319.
Mortensen, K., Y Tomkiewicz, T. D. Schultz, and E. M. Engler, 1981, Phys. Rev. Lett. **46**, 1234.
Mozurkewich, G., P. M. Chaikin, W. G. Clark, and G. Grüner, 1985, Solid State Commun. **56**, 421.
Nakamura, T., G. Saito, T. Inukai, T. Sugano, M. Kinoshita, and M. Konno, 1990, Solid State Commun. **75**, 583.
Ng, H. K., T. Timusk, and K. Bechgaard, 1984, Phys. Rev. B **30**, 5842.
Nomura, K., T. Shiizu, K. Ichimura, T. Sambongi, M. Tokumoto, H. Anzai, and N. Kinoshita, 1989, Solid State Commun. **72**, 1123.
Overhauser, A. W., 1960, Phys. Rev. Lett. **4**, 462.
Overhauser, A. W., 1962, Phys. Rev. **128**, 1437.
Pouget, J. P., 1993, private communication.
Psaltakis, G. C., 1984, Solid State Commun. **51**, 535.
Quinlivan, D., Y. Kim, K. Holczer, G. Grüner, and F. Wudl, 1990, Phys. Rev. Lett. **65**, 1816.
Sambongi, T. K. Nomura, T. Shimizu, K. Ichimura, N. Kinoshita, M. Tokumoto, and H. Anzai, 1989, Solid State Commun. **72**, 817.
Sham, L. J., and B. R. Patton, 1976, Phys. Rev. B **13**, 2151.
Shapiro, S., 1963, Phys. Rev. Lett. **11**, 80.
Shimizu, T., K. Nomura, T. Sambongi, H. Anzai, N. Kinoshita, and M. Tokumoto, 1991, Solid State Commun. **78**, 697.
Sneddon, L., 1984, Phys. Rev. B **29**, 719.
Solyom, J., 1979, Adv. Phys. **28**, 201.
Takada, T., 1984, J. Phys. Soc. Jpn. **53**, 2193.
Takahashi, T., D. Jérome, and K. Bechgaard, 1984, J. Phys. Lett. **45**, 945.
Takahashi, T., Y. Maniwa, H. Kawamura, K. Murata, and G. Saito, 1986a, Physica B **143**, 417.
Takahashi, T., Y. Maniwa, H. Kawamura, K. Murata, and G. Saito, 1986b, J. Phys. Soc. Jpn. **55**, 1364.
Tinkham, M., 1975, *Introduction to Superconductivity* (R. E. Kniegler, Malabar, Florida).
Tomić, S., J. R. Cooper, D. Jérome, and K. Bechgaard, 1989, Phys. Rev. Lett. **62**, 462.
Tomić, S., J. R. Cooper, W. Kang, D. Jérome, and K. Maki, 1991, J. Phys. (Paris) I **1**, 1603.
Torrance, J., H. J. Pederson, and K. Bechgaard, 1982, Phys. Rev. Lett. **49**, 881.
Trætteberg, O., G. Kriza, C. Lenoir, Y.-S. Huang, P. Batail, and D. Jérome, 1993, in Proceedings of the International Conference on Synthetic Metals, Göteborg, Sweden, 1992 (in press).
Trætteberg, O., G. Kriza, C. Lenoir, Y.-S. Huang, P. Batail, and D. Jérome, 1994, Phys. Rev. B **49**, 409.
Trætteberg, O., G. Kriza, and G. Mihály, 1992, Phys. Rev. B **45**, 8795.
Trætteberg, O., C. Lenoir, Y.S. Huang, G. Kriza, G. Quirion, P. Auban-Senzier, W. Kang, P. Batail, and D. Jérome, 1993, in Proceedings of the International Conference on Synthetic Metals, Göteborg, Sweden, 1992 [Synth. Met. **56**, 2785].
Tua, P. F., and J. Ruvalds, 1985, Phys. Rev. B **32**, 4660.
Tüttő, I., and A. Zawadowski, 1985, Phys. Rev. B **32**, 2449.
Tüttő, I., and A. Zawadowski, 1988, Phys. Rev. Lett. **60**, 1442.
Walsh, W. M., Jr., F. Wudl, G. A. Thomas, D. Nalewajek, J. J. Hauser, P. A. Lee, and T. Poehler, 1980, Phys. Rev. Lett. **45**, 829.
Wong, W. H., *et al.*, 1993, Phys. Rev. Lett. **70**, 1882.
Wonneberger, W., 1991a, Synth. Met. **41**, 3793.
Wonneberger, W., 1991b, Solid State Commun. **80**, 953.
Wu, Wei-yu, A. Jánossy, and G. Grüner, 1984, Solid State Commun. **49**, 1013.
Yamaji, H., 1982, J. Phys. Soc. Jpn. **51**, 2787.
Yamaji, H., 1983, J. Phys. Soc. Jpn. **52**, 1361.
Zawadowski, A., and I. Tüttő, 1989, Synth. Met. **29**, F469.
Zettl, A. and G. Grüner, 1982a, Phys. Rev. B **26**, 2298.
Zettl, A., and G. Grüner, 1982b, Phys. Rev. B **25**, 2081.
Zettl, A., and G. Grüner, 1984, Phys. Rev. B **29**, 755.